AN INVESTIGATION OF THE MECHANISM OF HEAT TRANSFER NEAR THE CRITICAL STATE OF A FLUID

Thesis by

Jerry D. Griffith

In Partial Fulfillment of the Requirements
For the Degree of
Mechanical Engineer

California Institute of Technology
Pasadena, California
1960

ACKNOWLEDGEMENTS

Professor R. H. Sabersky directed the project in all its phases and his guidance was deeply appreciated. Mr. Taras Kiceniuk and Mr. Don Laird aided the author in designing and constructing the experimental installation. Mrs. Ruth Toy and Mrs. Beverly McAllister assisted in the procurement of equipment and many of the other chores incidental to experimental work. To all of these persons the author wishes to express his gratitude for their time and effort spent in the various phases of the project.

ABSTRACT

Very large heat transfer coefficients have been observed in the one phase region near the critical point of some fluids. There has been some conjecture that the increase in these coefficients might be due to the agitation caused by bubble-like aggregates of low density fluid. It was believed that these bubble-like formations might grow and collapse in much the same way as actual bubbles in nucleate boiling. The purpose of these experiments was to see if the suggested mechanism of heat transfer could be observed and if it could be related to a significant increase in the heat transfer rate. Freon 114A was chosen as the test fluid because of its relatively low critical temperature and pressure. With this fluid and with the range of variables tested, bubble-like formations were observed under some conditions. However, no definite correlation to an increase in the heat transfer rate was noted. This fact should not exclude the possibility that bubble-like activity might result in a sharp increase in heat transfer rates in other fluids or even under different operating conditions with the fluid in question.

TABLE OF CONTENTS

I. INTRODUCTION

The critical state of a fluid is specified by that temperature and pressure above which a fluid in equilibrium can no longer exist simultaneously as a liquid and vapor. If either of the quantities, temperature or pressure, are held at or above the critical value, the fluid cannot be made to pass through a two-phase region.

Below the critical state of a fluid heat can be transferred to a fluid by normal convection, nucleate boiling, partial film boiling, or complete film boiling. In the nucleate boiling region the heat transfer coefficient h ($Btu/in^2\ sec\ ^oF$) is many times higher than in the other regions. This increase is generally attributed to the agitation caused by the motion of vapor bubbles which grow on the heating surface and either collapse or move out into the fluid.

Above and near the critical state abrupt increases in heat transfer rates and heat transfer coefficients have also been observed in some fluids. (1) (2) (3) (4) (5). This rise in the heat transfer coefficient cannot be attributed to the growth of bubbles in the ordinary sense, since two phases cannot exist above the critical state. However, various papers (3) (4) have suggested that the increase might be attributed to the agitation caused by bubble-like aggregates of low density fluid which might grow near the surface of the heating element and move into the relatively high density bulk fluid and collapse. The purpose of this investigation was to measure the heat transfer rates to a fluid near its critical state and to take Schlieren photographs to see if such an increase in the heat transfer coefficient could be observed and if it could be correlated to bubble-like activity.

II TEST PROGRAM

Freon 114A was selected as the test fluid because of its relatively low critical temperature and pressure. (See Appendix F for a table of Significant Properties of Freon 114A.)

A 0.010 in. Nichrome wire was selected as the heat transfer element. The values of thermal coefficient of resistivity, α, and resistance, R, of Nichrome are such that an accuracy acceptable for the present purpose could be obtained. For a given length of wire it is desirable to have both α and R as high as possible since wire temperature is measured by a change in resistance of the wire, and for a given temperature change ΔR is larger for larger values of R and α.

The test fluid was pressurized by means of a high pressure nitrogen bottle connected to the cylinder containing the test fluid through a regulator. Consequently, the Freon 114A would be saturated with nitrogen and the results obtained must be examined with this in mind. Equipment was obtained and constructed to measure the heat transfer rates and wire temperature so that graphs of the heat transfer rate, q, vs. wire temperature, T_w, and of the heat transfer coefficient, h, vs. wire temperature, could be plotted. Photographs were taken corresponding to various stations on the two types of graphs.

The above information was used to determine if sharp increases in q or h vs. T_w curves existed and if so, to examine if such increases could be related to bubble-like activity.

It was realized that the results would apply only to the fluid and conditions under test. For example, should no bubble-like activity be observed beyond the critical point, this would by no means indicate that such activity did not exist under different test conditions or for different fluids.

III. TEST INSTALLATION

The apparatus for this experiment may be divided into three systems, each one of which is illustrated in a separate diagram. A photograph of the combined setup shows how these three systems are inter related. (See fig. 1.)

The Pressure System was constructed as shown in fig. 2. Pressure was supplied to the system by means of a nitrogen bottle with a maximum pressure of 2200 psi. A pressure regulator served to reduce the pressure of the nitrogen in the bottle to the required operating pressure, and to maintain pressure at any desired value below 1500 psi. Two pressure gauges were mounted on the regulator to read the input and output pressures respectively. The output gauge was tested and found to be accurate to within ±10 psi. Since no higher accuracy was necessary for the experiment, there was no need to have a more accurate gauge mounted closer to the test cylinder. Pressure was transmitted to the fluid tested by means of 1/4 in. copper tubing. A surge tank was introduced into the pressure line to provide a cushioning effect for any pressure fluctuation in the test cylinder due to rises in temperature of the fluid. The test cylinder was made of regular Shelby steel tube 3 in. OD x 2 in. ID x 5-1/2 in. long. Detailed description of this part and complementary elements can be obtained from the enclosed drawing (fig. 3). A 2-1/8 in. diameter x 1 in. thick quartz crystal window was mounted on each end of the test bomb (see fig. 3).

The Electrical System is illustrated in fig. 5. Power was supplied to the test wire from a 120 volt DC power outlet through a rheostat made by the Ward Leonard Electric Company, Mt. Vernon, New York, Type 16106-6, Class 4253. This rheostat had 40 settings from 0.5 to 100.5 ohms and could be used to draw 1.17-45.8 amps at 120 volts. A 0-15 amp triplet ammeter, Model 0321-T, was obtained to measure the current through the test wire. Under test conditions it was found that the desired current range was smaller than anticipated and an alternate method of calculating the current through the test wire was used. (See Appendix C for a sample calculation.) The ammeter

was then used only as a reference. To measure the change in resistance of the test wire, a Wheatstone Bridge was constructed with one of the legs of the bridge being the test wire. Three legs of the bridge were made out of manganin wire with a resistance approximately equal to that of the test wire, and with a length 20 times and a diameter 2-1/2 times that of the test wire. These three legs were submerged in non-conducting transformer oil to keep the temperature change of the wire at a minimum. Manganin has a thermal coefficient of resistivity of less than 0.000001 ohms/ohm ^{o}C at 25 ^{o}C and more than -0.000042 ohms/ohm ^{o}C at 100 ^{o}C (6). These values compared to the value of the coefficient of resistivity for Nichrome 0.000170 ohms/ohm ^{o}C (7) insured that the change in resistance of the bridge elements would not be great enough to affect the measurement of the change in resistance of the test wire. One leg of the bridge was made with a resistance 0.050 ohms less than that of the test wire. Three parallel lengths of manganin wire with a combined resistance of approximately 0.100 ohms and a length of 1-1/2 ft. were added in series to this leg. This series resistance could be varied by a sliding contact to balance the bridge. The galvanometer used in the Wheatstone Bridge circuit was a Dejur microammeter, Model S-310, with a range of 0-100 microamperes and an internal resistance of 978 ohms. A Nichrome test wire 1.0 in. long with a measured resistance of 0.600 ohms was mounted on a capsule made out of two asbestos-cement plates. The capsule could be inserted into the test cylinder and held in place by reworked spark plugs. The spark plugs also provided an electrical circuit into the test cylinder and through the test wire by means of pressurized contacts as demonstrated in fig. 3. A picture of the capsule is also shown in fig. 4. An Iron-Constantan thermocouple was taped to the inner diameter of the end lock screws near the quartz windows. This gave a fairly accurate measurement of the fluid temperature since the cylinder was heated from the outside by infra red lamps. Heating was very slow and equilibrium was easy to maintain. The thermocouple was connected to

a Leeds Northrup potentiometer, Model 515588, with a range 0-850 ^{o}F. This potentiometer read directly in degrees fahrenheit and had a cold junction compensation which eliminated the need for a constant temperature ice bath.

The Optical System is illustrated in fig. 6. A point source of light was obtained by using a 6 volt - 18 amp ribbon filament microscope illuminator in conjunction with a transformer. The light was mounted so that the ribbon was vertical. This gave more illumination when the source was focused on a slit to form a line source for the Schlieren effect. A slit source was obtained by focusing the light source on two razor blades separated approximately 0.010 in. and mounted upright in the position shown in fig. 6. The light source was focused on the slit by using a f/4.7 127mm achromatic lens. This lens was taken from the camera and the camera was used without an additional lens. The light from the slit source was rendered parallel to go through the test cylinder by means of a 9 in. focal length projector lens made by the Buhl Optical Company, Pittsburgh, Pennsylvania. The light emerging from the test cylinder was focused on a sharp edge by means of a 9 in. focal length projector lens identical to the one listed above. The sharp edge necessary to give the Schlieren effect was made with a razor blade mounted upright and parallel to the slit source and located at the point where the light converged from the 9 in. focal length projector lens. A 4 x 5 Graflex Speed Graphic Camera, Serial No. 455529, was used to photograph the wire under test conditions. The camera was used without lens to obtain the magnification desired. With the above arrangement the magnification was approximately 12.5:1 and could be varied by varying distances E and G in fig. 6. Fig. 6 also shows the various separation distances of the optical equipment as it was located under test. These distances must be considered as approximate since a very accurate adjustment is necessary to obtain the Schlieren effect. An optical bench was constructed by using wooden blocks drilled simultaneously to be centered by two 7/16 in. diameter cold-rolled steel rods. Holes to

mount the optical equipment were simultaneously center-drilled to insure alignment, and set screws were provided to position the optical equipment securely after it was properly adjusted. Steel rods were mounted on top of the wooden blocks and the entire test installation from light source to camera was enclosed with black cloth to make a light tunnel during the test.

IV. TEST PROCEDURE

The Wheatstone Bridge was calibrated as shown in Appendix B, and with the equipment in position as shown in fig. 1, the test cylinder was filled with Freon 114A. Since Freon 114A boils at 37.6 ^{o}F at atmospheric pressure, it was first necessary to cool both the test cylinder and the vessel containing the Freon before the Freon could be poured into the test cylinder. With the cylinder full, pressure was applied by opening the regulator. The room temperature during the first test was 80 ^{o}F so the test fluid was heated back up to this temperature. The Wheatstone Bridge did not have sufficient sensitivity to balance the bridge with a small current flowing through it. The error in such a balance would be large (at least 14 ^{o}F) and this error would be multiplied in subsequent tests by the ratio of the current flowing through the test wire to the balance current. This ratio could be as high as 6:1. To provide a proper initial setting of the bridge, the fluid pressure was adjusted to 350 psi where the boiling point was known to be 265 ^{o}F. With the fluid bulk temperature at 80 ^{o}F, the current through the test wire was increased until boiling was observed. The bridge was then adjusted so that it gave a calculated wire temperature of 265 ^{o}F. The adjustment was checked by making a similar observation at 200 psi where the boiling temperature was known to be 214 ^{o}F. With the bridge adjusted, test runs were made at fluid bulk temperatures of 80 ^{o}F and pressures of 200, 350, and 550 psi. Then with the pressure set at 550 psi, test runs were made with fluid bulk temperatures of 150, 200, 285, 300 and 350 ^{o}F.

The data which were recorded were the current flowing through the wire in amperes and the unbalance of the bridge in microamperes. This information was sufficient to construct graphs of heat transfer rate and heat transfer coefficient vs. wall temperature for these various test runs. At various points during each run, photographs were taken so that the heat transfer rate and heat transfer coefficient could be correlated to the mechanism of heat transfer.

V. RESULTS

In figs. 7 through 14 graphs are shown of the heat transfer rate q (BTU/in^2 sec) and the heat transfer coefficient h (BTU/in^2 sec-$^\circ$F) vs. wire temperature. Mounted on the page opposite each graph are Schlieren photographs of the convection currents around the wire. The photographs are numbered and the same number is used on the graphs to indicate the point at which the photograph was taken. For the first photograph, fig. 7, a picture of the unheated test wire is shown for reference. Individual graphs are shown for each of the following test runs:

Set No.	Figure No.	Pressure (psi)	Bulk Fluid Temperature ($^\circ$F)
I	7	200	80
II	8	350	80
III	9	550	80
IV	10	550	150
V	11	550	200
VI	12	550	285
VII	13	550	300
VIII	14	550	350

The results of these individual tests are collected in two graphs. One graph, fig. 15, shows a plot of the heat transfer rate, q (BTU/in^2 sec) vs. wire temperature ($^\circ$F), and a second graph, fig. 16, shows a plot of the heat transfer coefficient, h (BTU/in^2 sec-$^\circ$F) vs. wire temperature T_w. Following the presentation of the data is a discussion of the information obtained.

Experimental Sets I and II were taken at pressures below the critical. Both Sets show the characteristic increase in q and h vs. T_w curves which is attributed to boiling. It is noted that bubbles are visible on the photographs which were taken at wire temperatures higher than the boiling temperature. Photographs corresponding to lower wire

temperature do not show any evidence of vapor bubbles with the exception of photograph no. 6 on which are seen cavities which have the general appearance of vapor bubbles. However, these cavities are believed to be largely made up of gas because they did not grow and collapse and behaved very similarly to the air bubbles which have been previously observed on heated surfaces in saturated liquids. (8) Furthermore, it is significant that these cavities appear only on the top of the wire, whereas bubble formations appear on the bottom of the wire also when boiling is occurring. The fact that the indicated boiling in the photograph correlates very well with the sharp increase in the curve of heat transfer rate vs. wire temperature is taken as an indication that the experimental setup is suitable for the purpose for which it was intended.

Experimental Sets III through VIII were taken at pressures above the critical (reduced pressure $P/P_{cr} = 1.15$). Sets III, IV, and V for which the fluid bulk temperatures were more than 90 ^{o}F below the critical value and Set VII for which the fluid bulk temperature was 6^{o} above the critical value have a common characteristic. The curves of heat transfer rates vs. wall temperature increase monotonically and no sharp changes in slope are noticed. For Sets III, IV, and V the heat transfer coefficient increases gradually until the wire reaches a temperature above critical and then remains relatively constant.

For Set VII the wire temperature is always above the critical value and the heat transfer coefficient remains relatively constant, at least in the region where it could be determined with the necessary accuracy. No sharp increases in the heat transfer coefficient are observed and no bubble-like activity was noted for wire temperatures near the critical temperature. For temperature differences between the wire and fluid of the order of 300 ^{o}F, however, Sets III and VII do show the growth of bubble-like low density regions near the wire surface. The bubble growth is quite violent and the low density regions burst into the bulk fluid. This heat transfer mechanism when viewed on the ground glass of the camera looked very much like the boiling which had been viewed at pressures below the critical. However, no abrupt changes in

the heat transfer rate or in the heat transfer coefficient occurred. Apparently the bubble-like activity was not providing any better circulation than the more common convection patterns.

There was one additional region in which bubble-like formations were observed, and this was the region for which both the temperature of the wire and that of the fluid were close to the critical value. Photograph No. 67, which corresponds to point 67 on fig. 12, is typical of this region. As can be seen from fig. 12, once again the occurrence of bubbles did not result in the sharp increase in heat transfer rate which is so characteristic of boiling heat transfer. An examination of the heat transfer coefficient is more difficult in this region as the values of ΔT are small, and the limit in accuracy in the temperature measurements leads to large uncertainties in h. Nevertheless, even if a local increase in h were to exist for this limited range of wire temperatures, it would, from an engineering point of view, be of only secondary importance since it is the obtainable heat transfer rate which is of primary interest.

Experiment Set VIII showed the free convection patterns expected in the super-critical region. The heat transfer rate and the heat transfer coefficient are noticeably less than in all the previous Sets.

VI. CONCLUSION

For the conditions under which tests were made, it may be concluded that for a reduced pressure of 1.15 no bubble-like activity and no sharp increase in the heat transfer rate or coefficient was observed as long as the fluid temperature was significantly below the critical value and as long as the temperature difference between the wire and fluid was below about 300 °F. For higher temperature differences, bubble-like activity could be observed. Such activity was, however, not associated with any significant increase in the heat transfer rate. It was furthermore observed that when the temperature of the fluid and of the wire were within about 9 °F. of the critical temperature, bubble-like activity seemed to exist. This activity again did not lead to any abrupt increase in the heat transfer rate. In addition to bubble-like formations, other types of complicated convection patterns were observed for fluid bulk temperature and wire temperature near the critical value. These patterns may well be of great significance in determining the heat transfer conditions. Their study may possibly serve as the subject of future investigation. The results shown are applicable only to the fluid in question and under the prevailing conditions of test. The fact that no increase in the heat transfer rate was noted for the bubble-like activity which was present during these tests should not exclude the possibility that bubble-like activity might be responsible for a sharp increase in heat transfer rates in other fluids or even in the same fluid, possibly at reduced pressures nearer to 1.0.

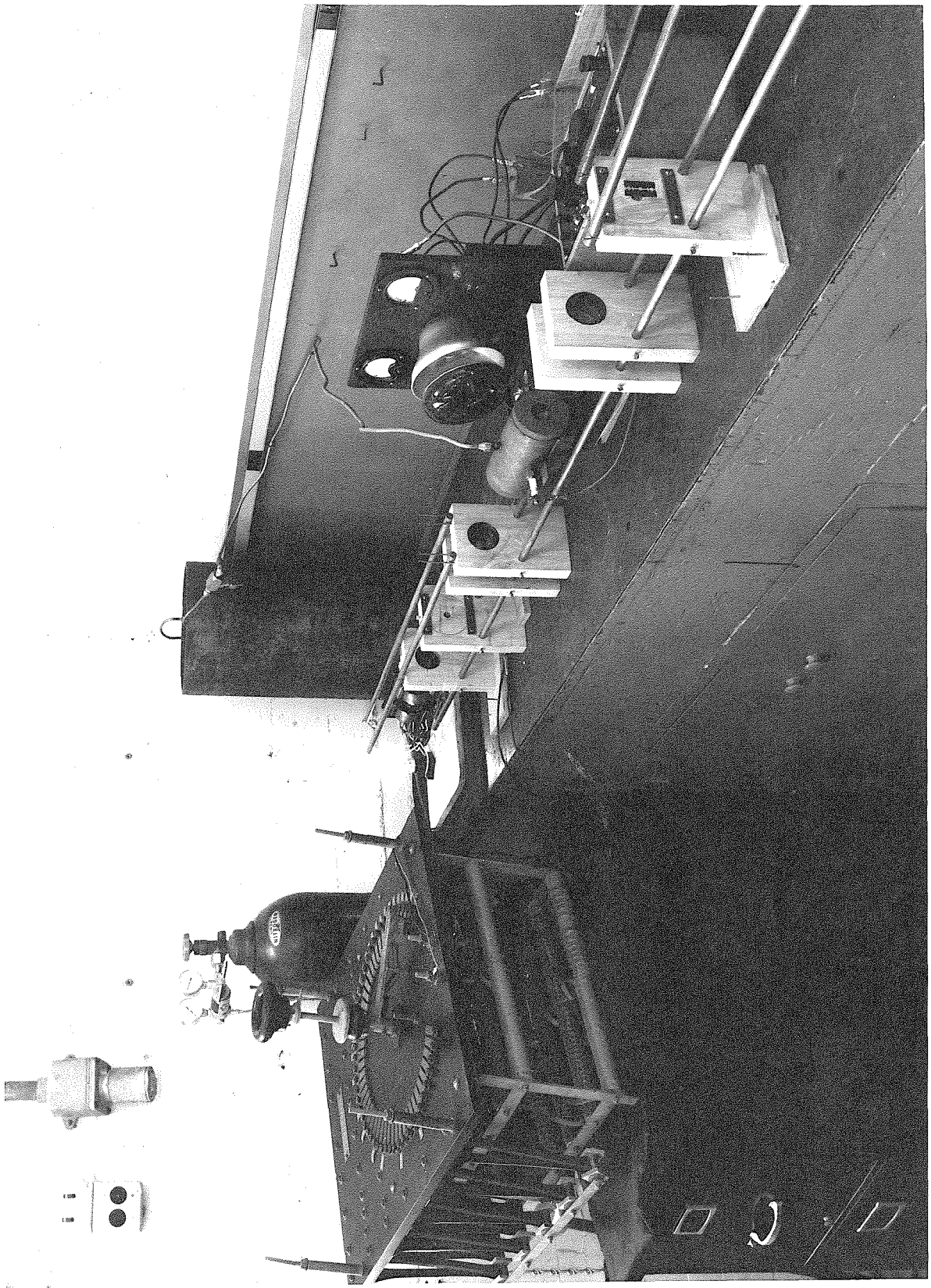

FIGURE 1

THE TEST INSTALLATION

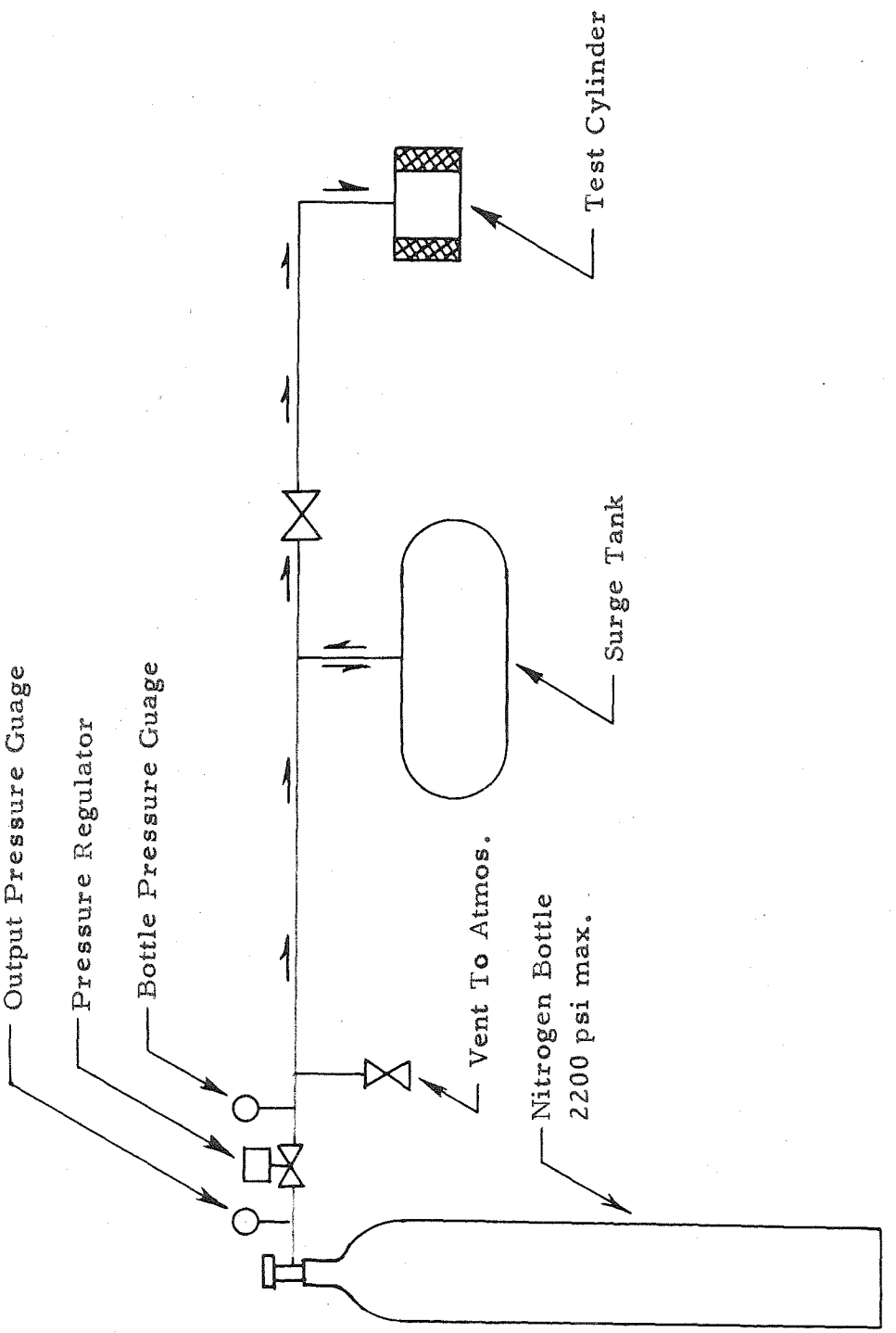

FIGURE 2

THE PRESSURE LINE DIAGRAM

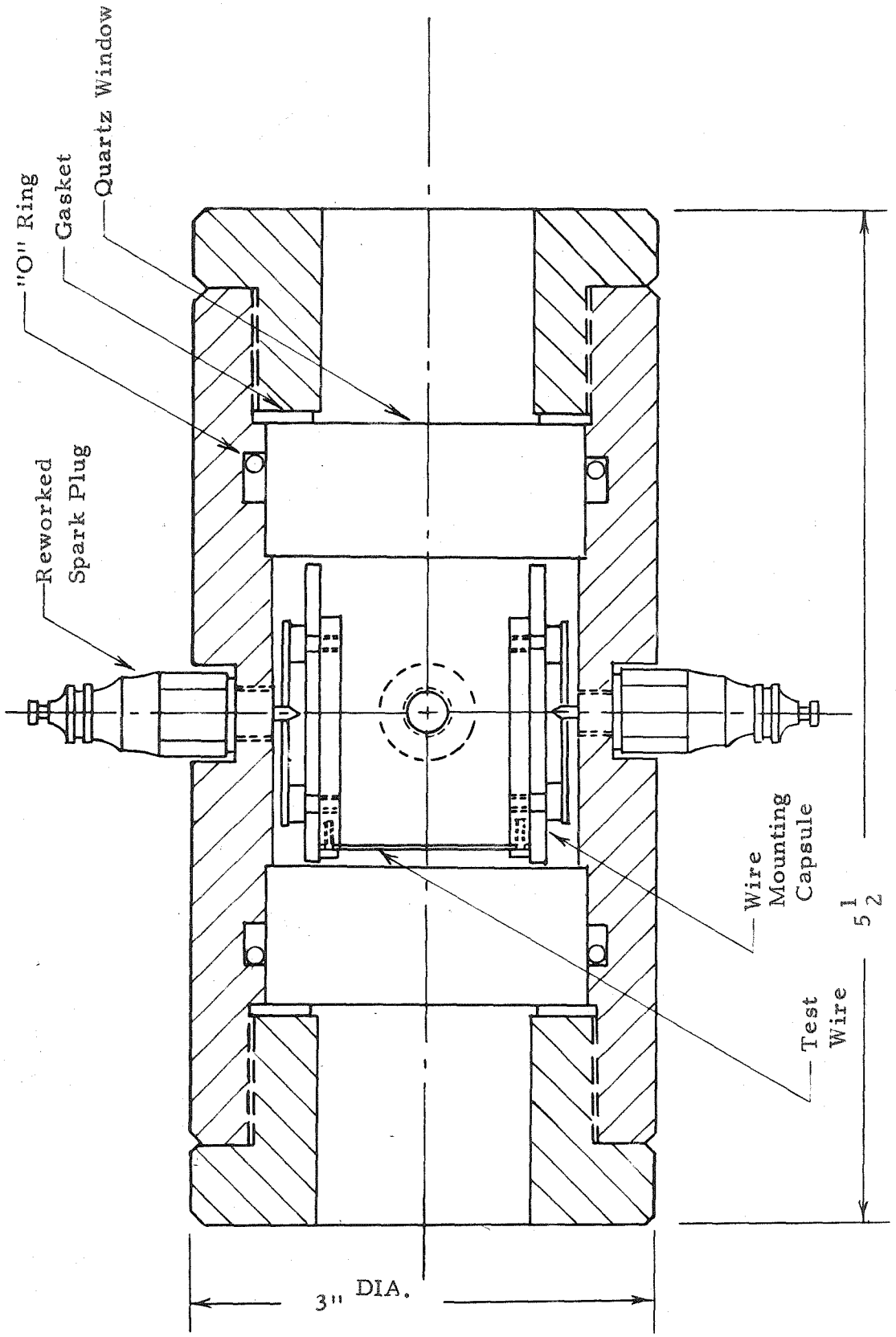

FIGURE 3

THE TEST CYLINDER

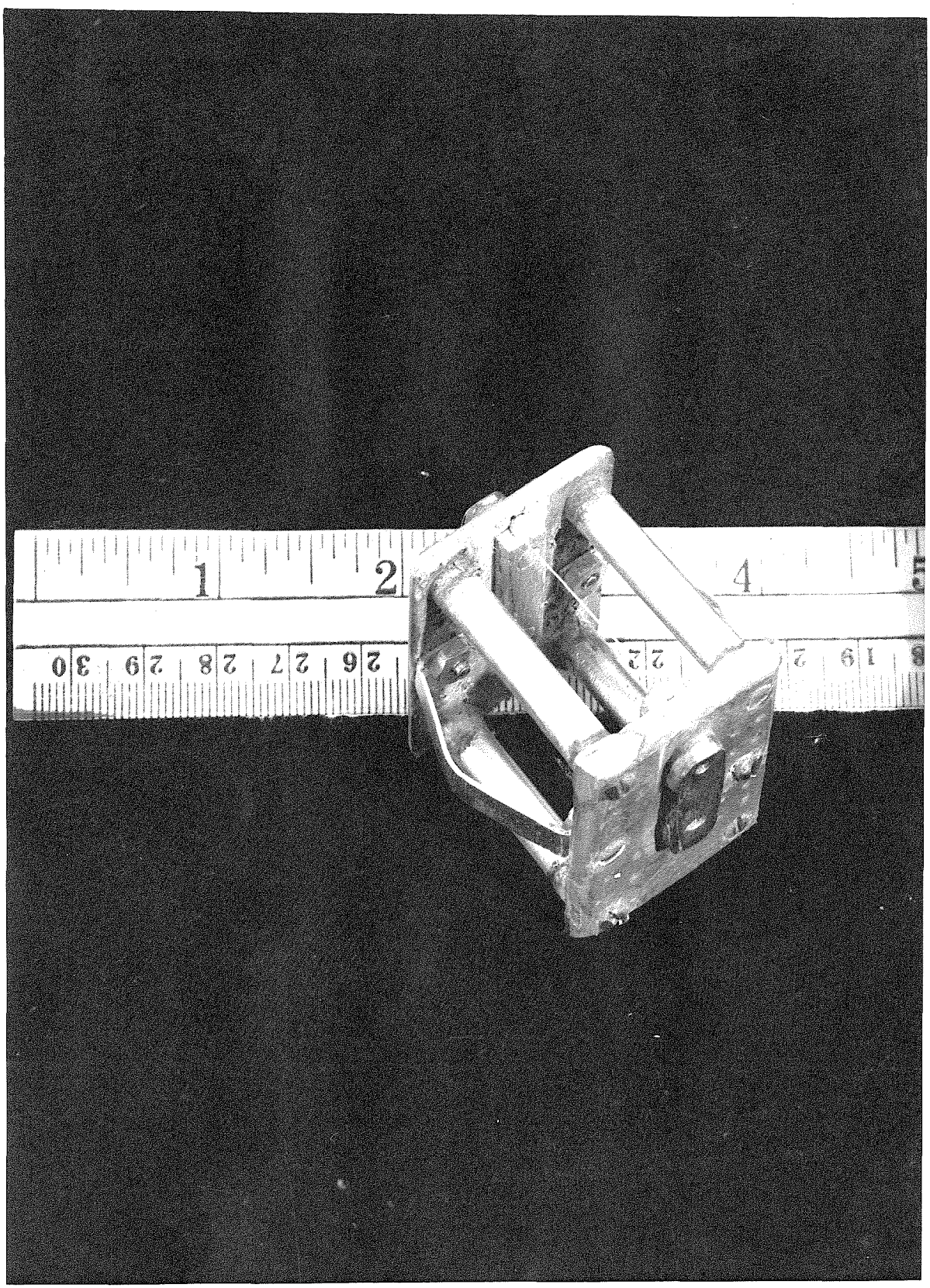

FIGURE 4

THE WIRE MOUNTING CAPSULE

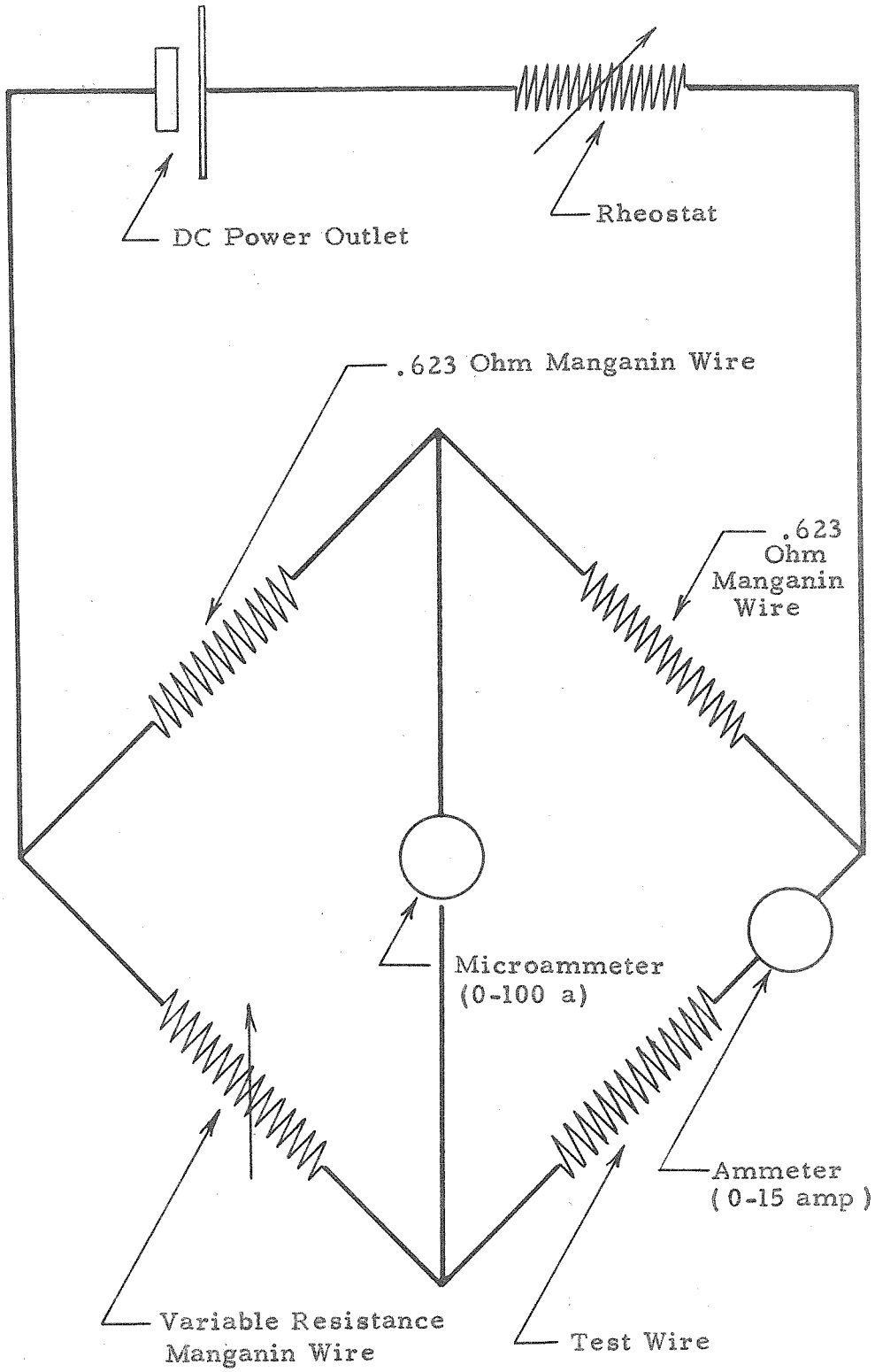

FIGURE 5

WIRING DIAGRAM

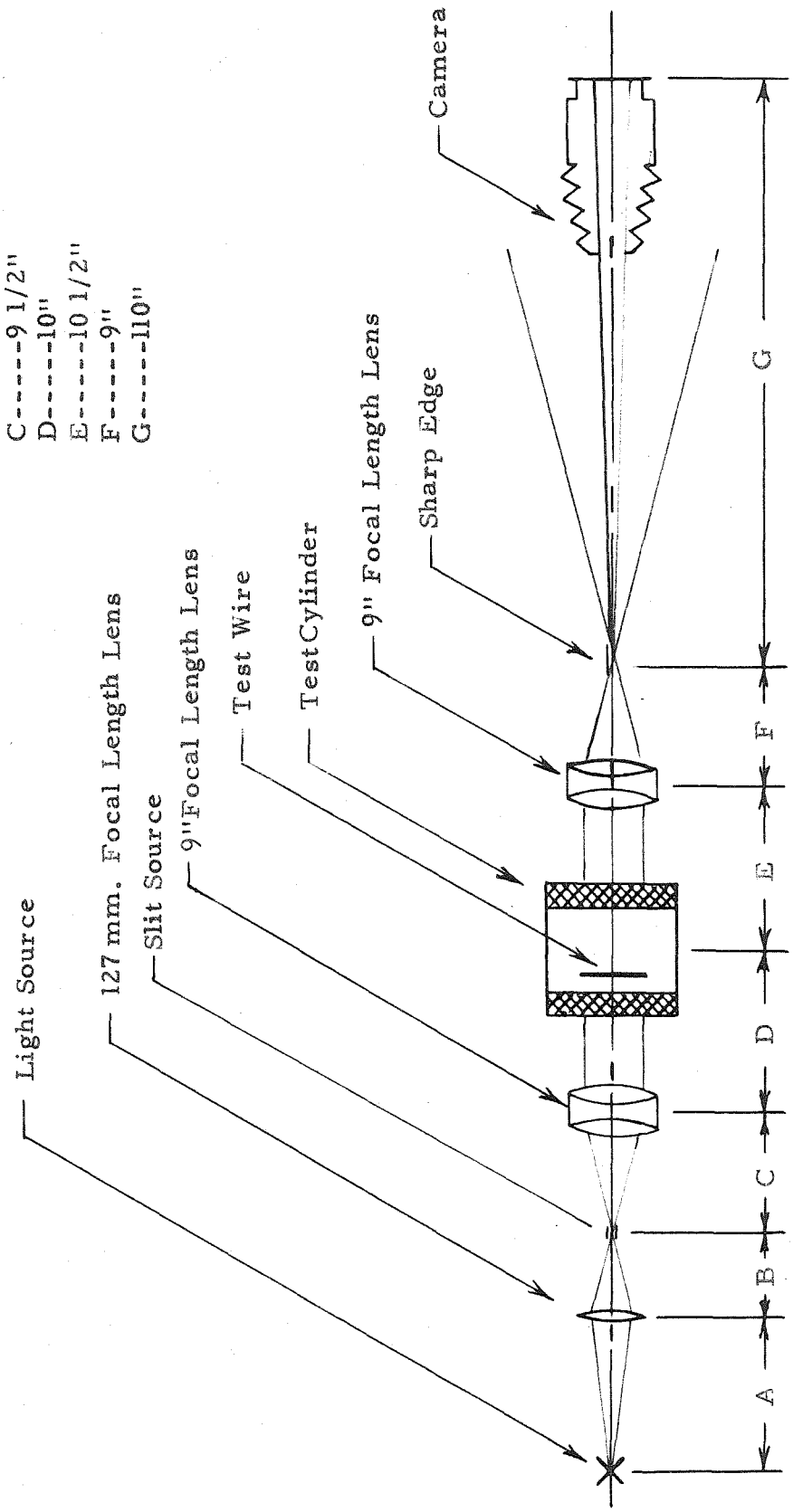

FIGURE 6

THE OPTICAL SYSTEM

TEST RESULTS

Set I

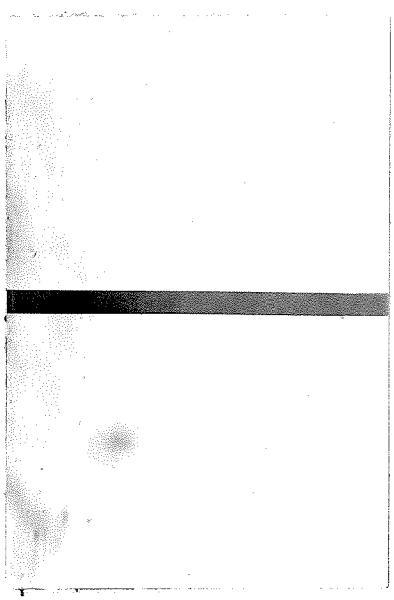

Unheated Test Wire

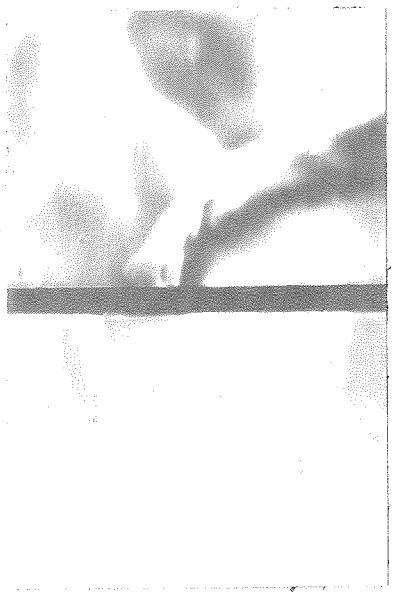

Station No. 2

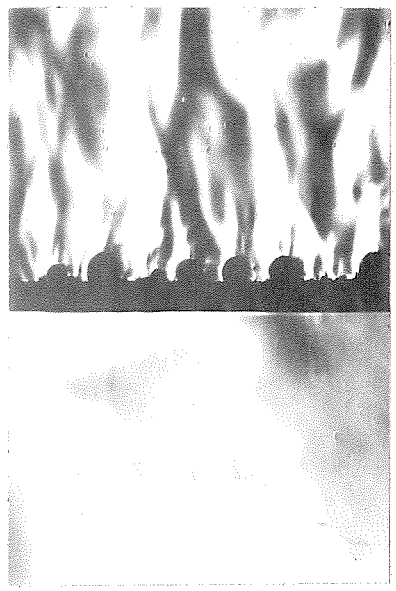

Station No. 6

Station No. 7

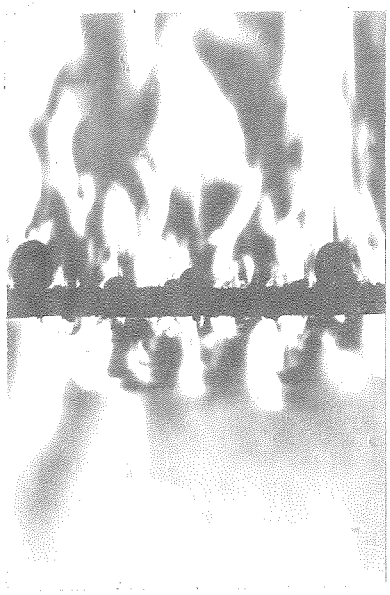

Station No. 8

Station No. 13

FIGURE 7

HEAT TRANSFER RATE & HEAT TRANSFER COEFFICIENT
vs. WIRE TEMPERATURE

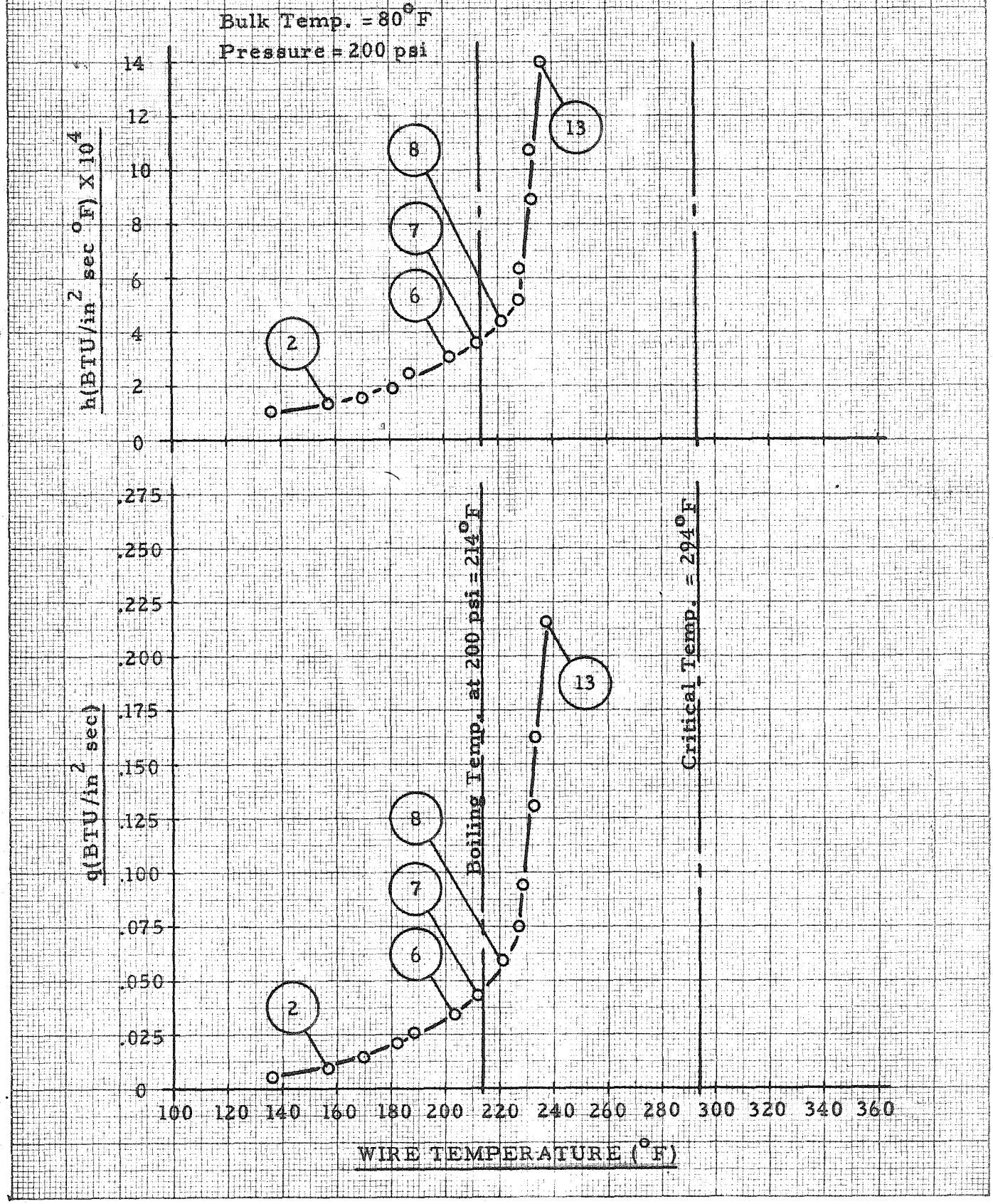

TEST RESULTS

Set II

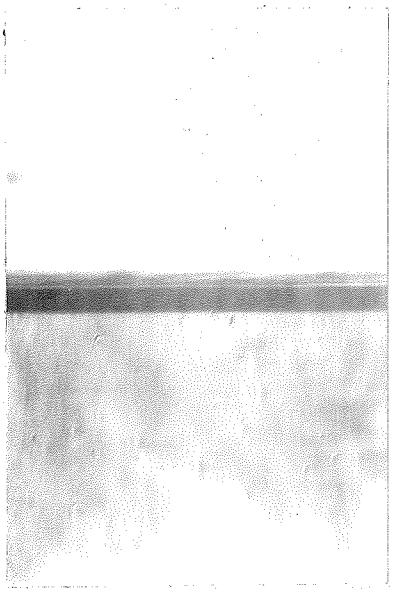

Station No. 19

Station No. 21

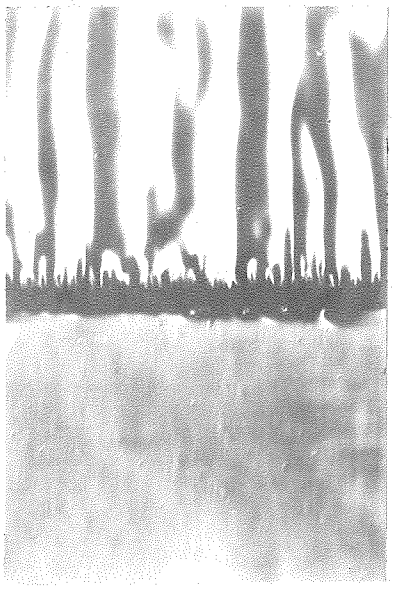

Station No. 22

Station No. 26

Station No. 27

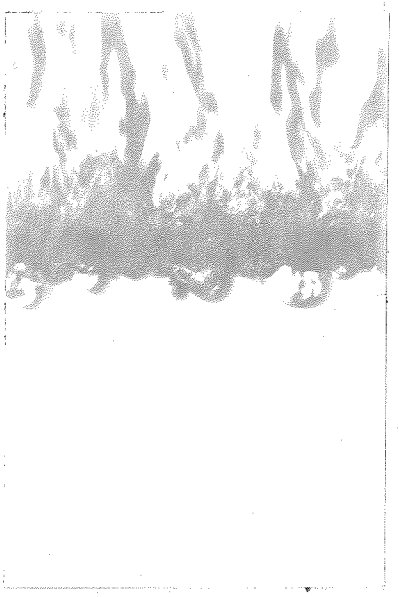

Station No. 28

FIGURE 8

HEAT TRANSFER RATE & HEAT TRANSFER COEFFICIENT
vs. WIRE TEMPERATURE

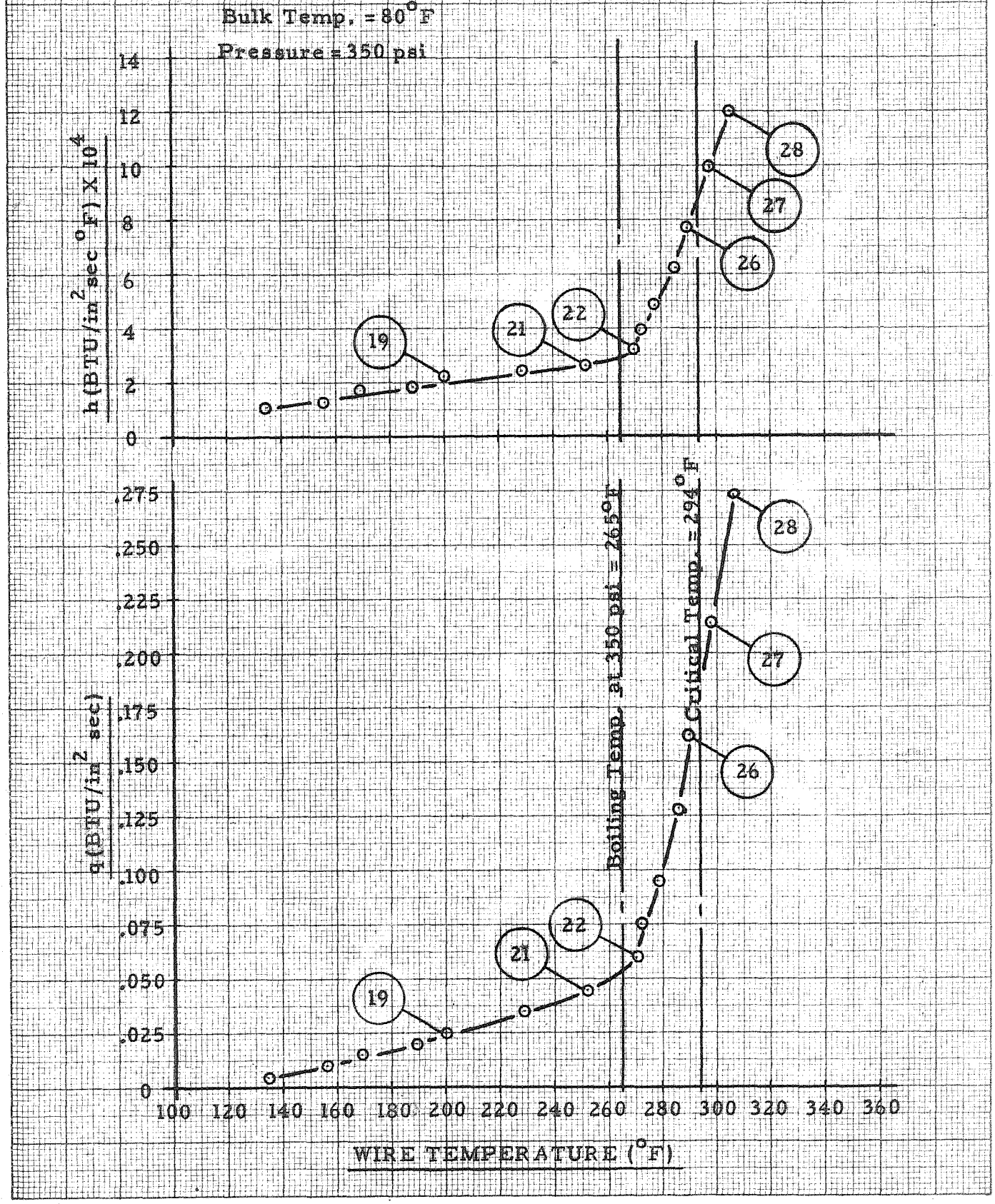

TEST RESULTS

Set III

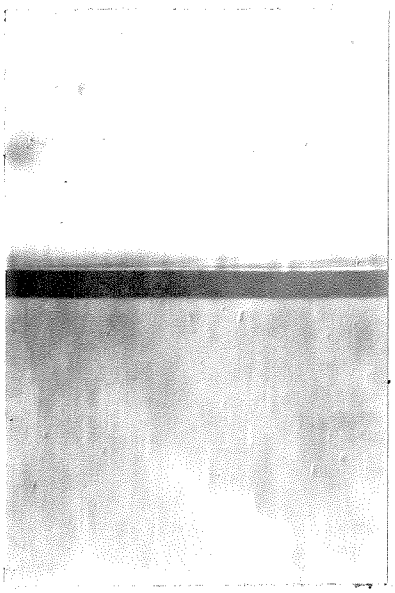

Station No. 36

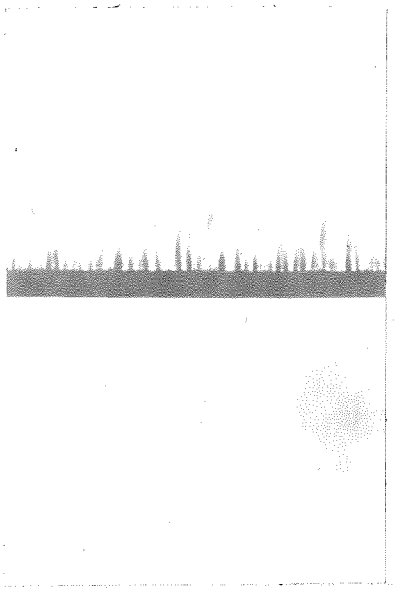

Station No. 37

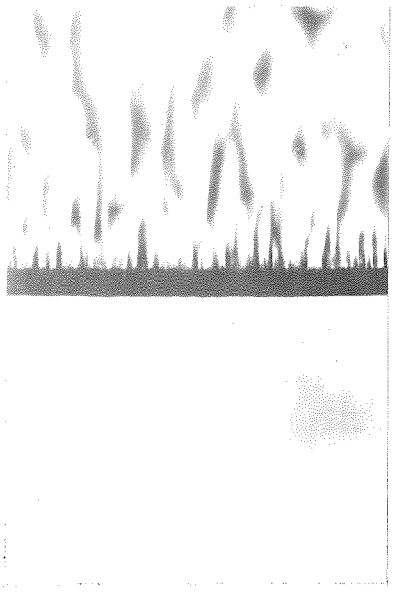

Station No. 38

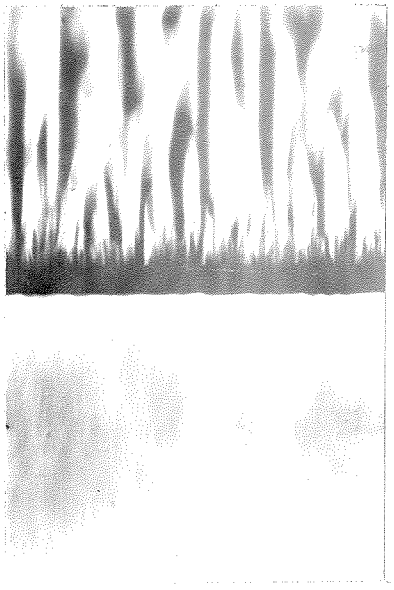

Station No. 39

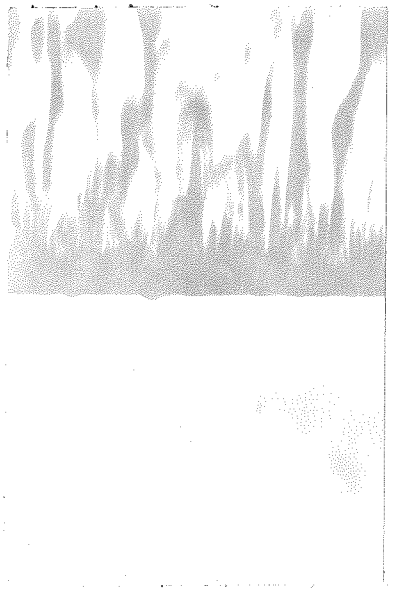

Station No. 40

Station No. 41

FIGURE 9

HEAT TRANSFER RATE & HEAT TRANSFER COEFFICIENT
vs. WIRE TEMPERATURE

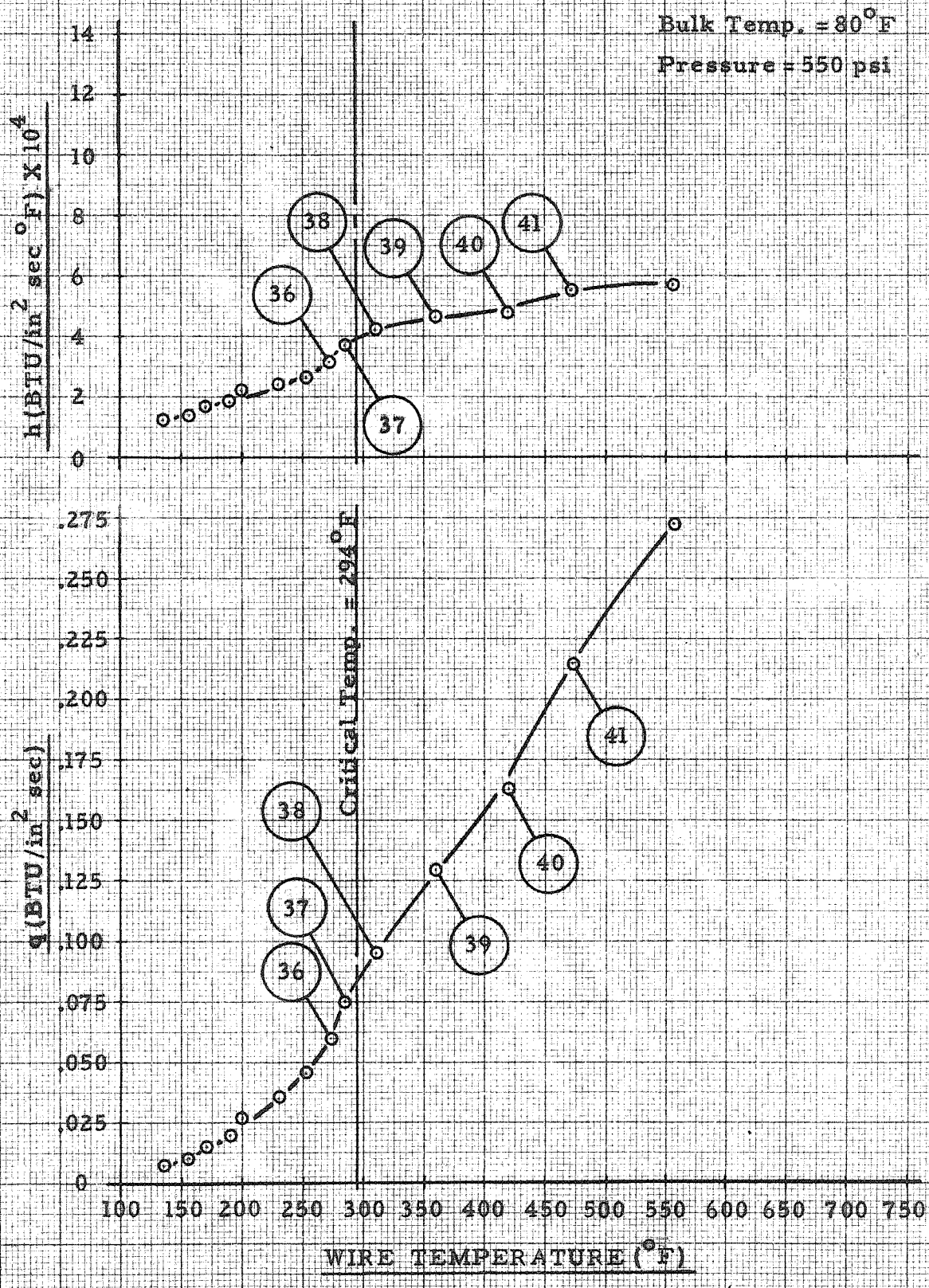

TEST RESULTS

Set IV

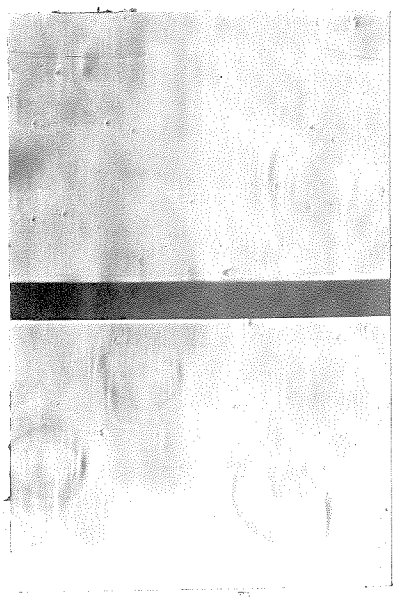

Station No. 45

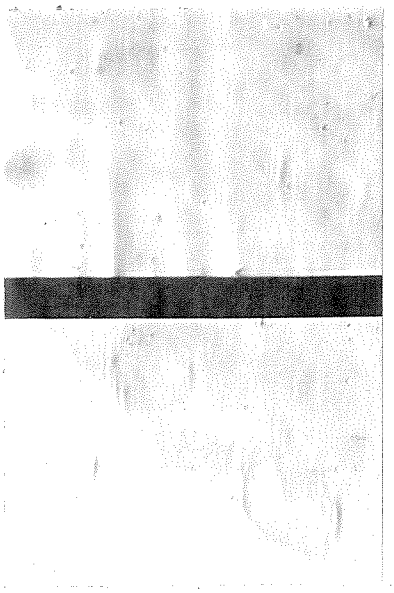

Station No. 48

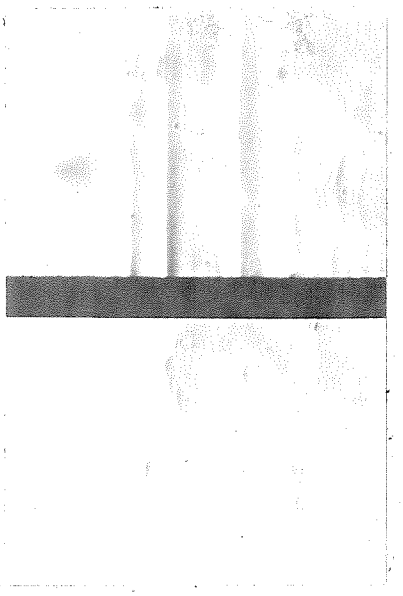

Station No. 50

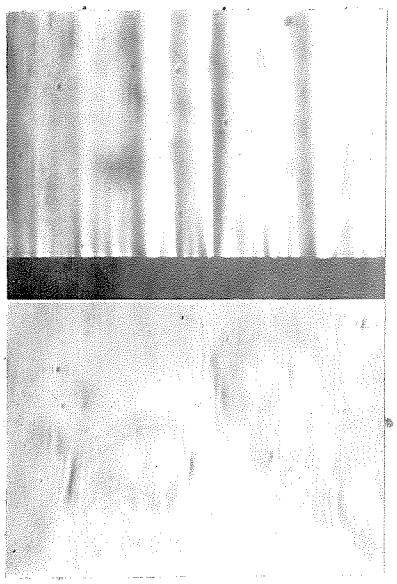

Station No. 52

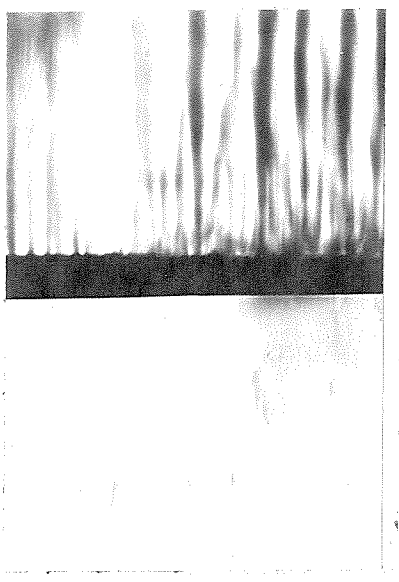

Station No. 53

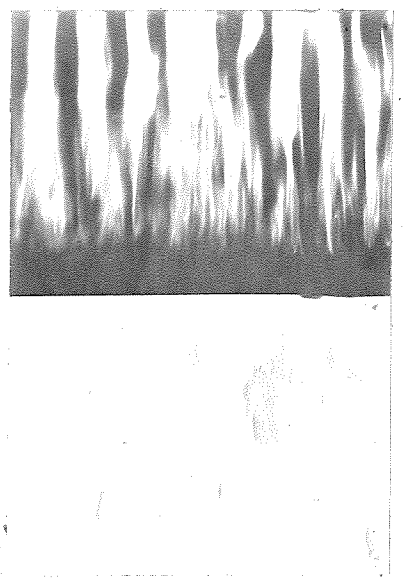

Station No. 54

FIGURE 10

HEAT TRANSFER RATE & HEAT TRANSFER COEFFICIENT
vs. WIRE TEMPERATURE

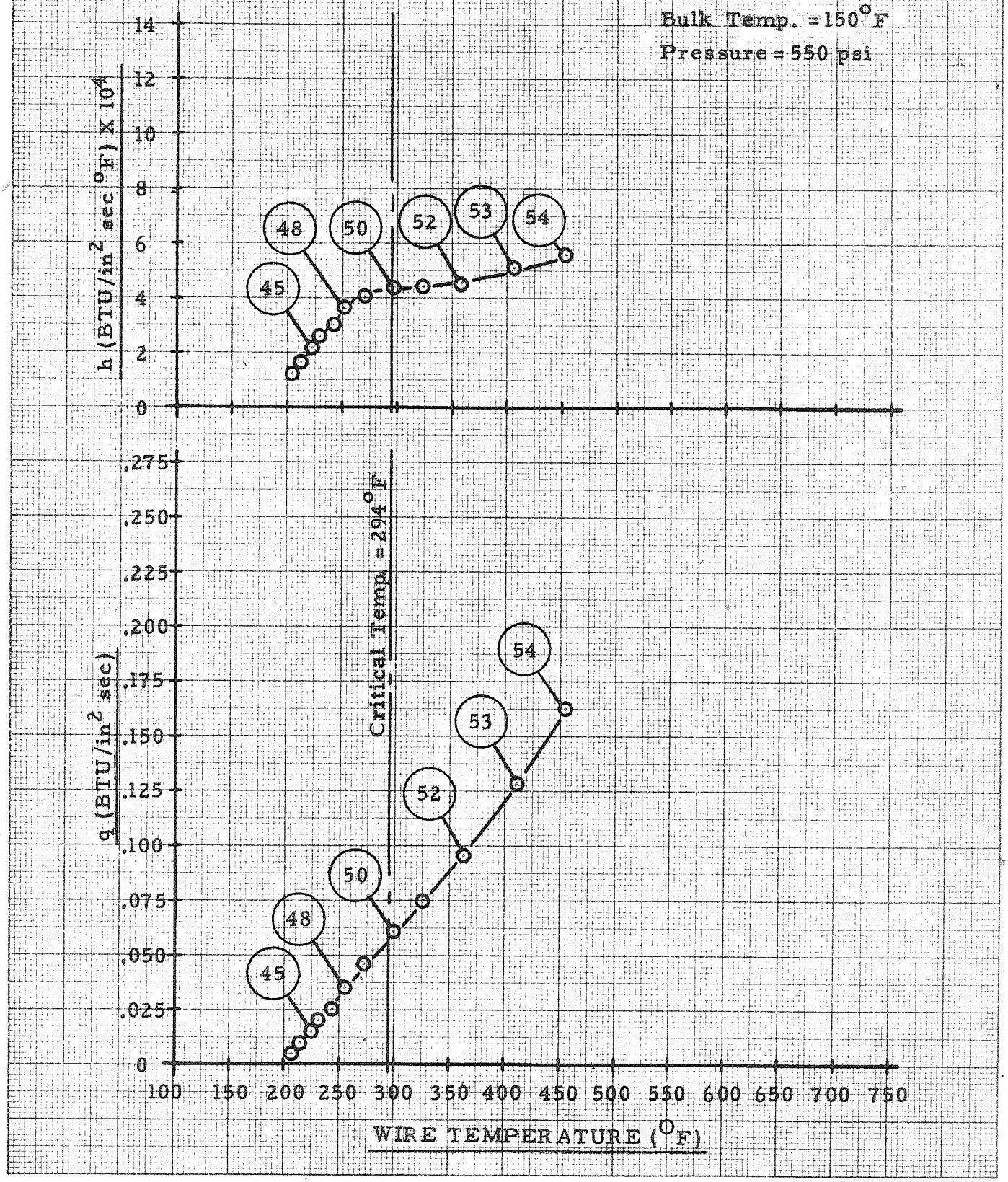

TEST RESULTS

Set V

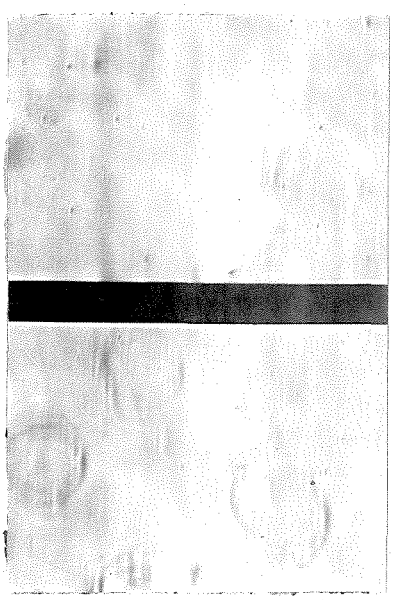

Station No. 57

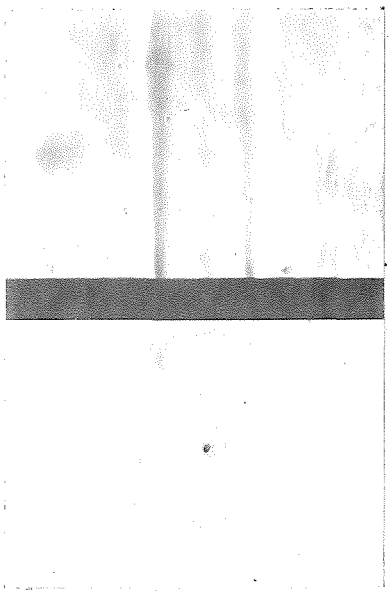

Station No. 60

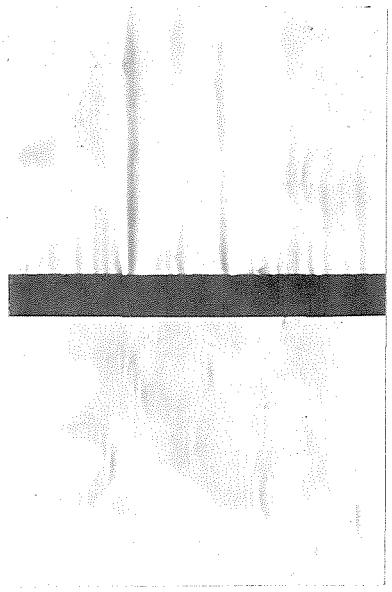

Station No. 62

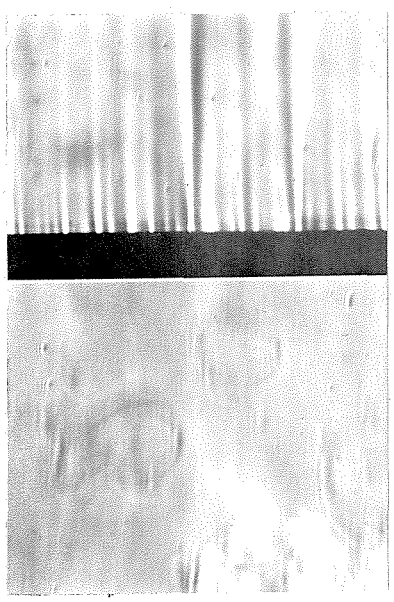

Station No. 64

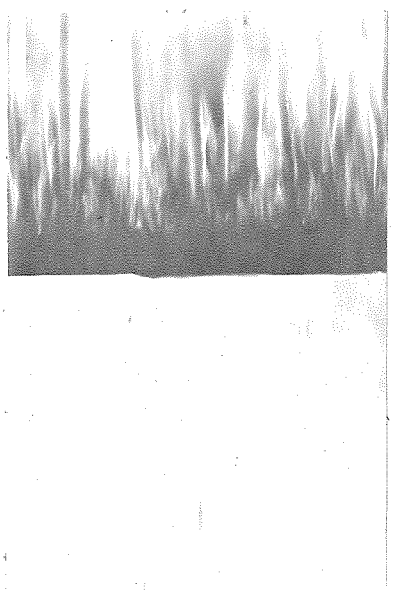

Station No. 65

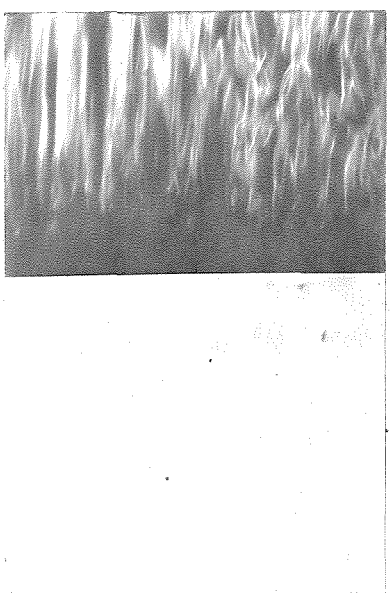

Station No. 66

FIGURE 11

HEAT TRANSFER RATE & HEAT TRANSFER COEFFICIENT
vs. WIRE TEMPERATURE

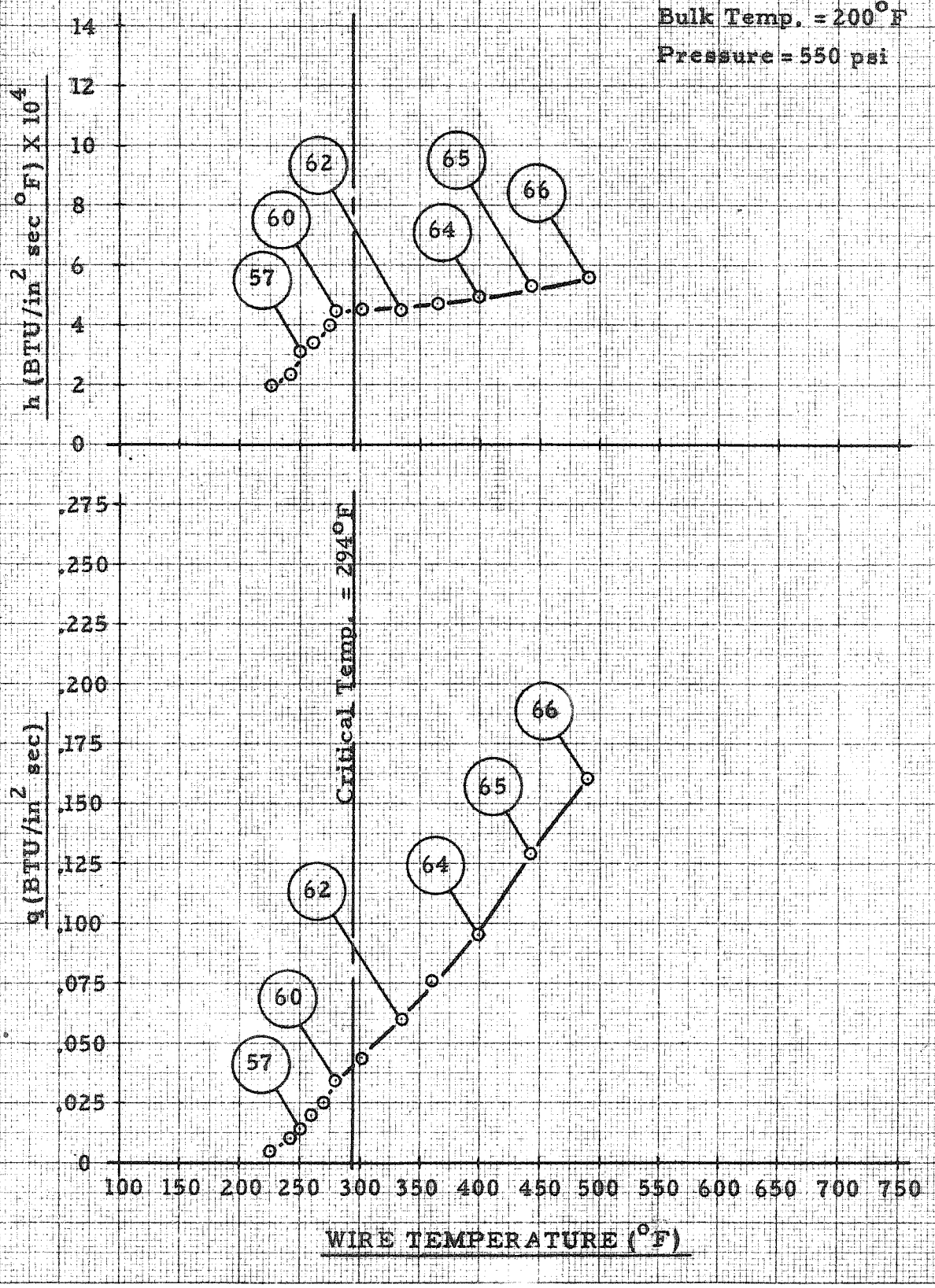

TEST RESULTS

Set VI

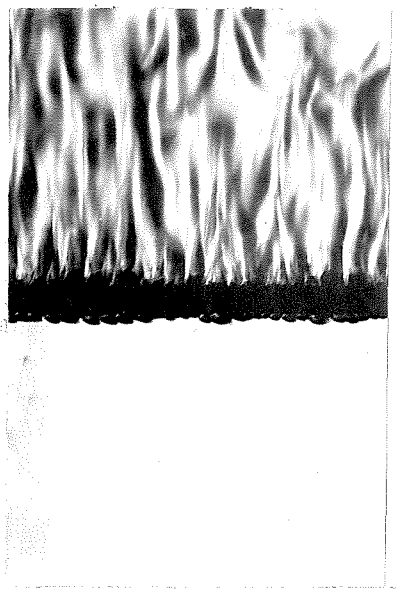

Station No. 67

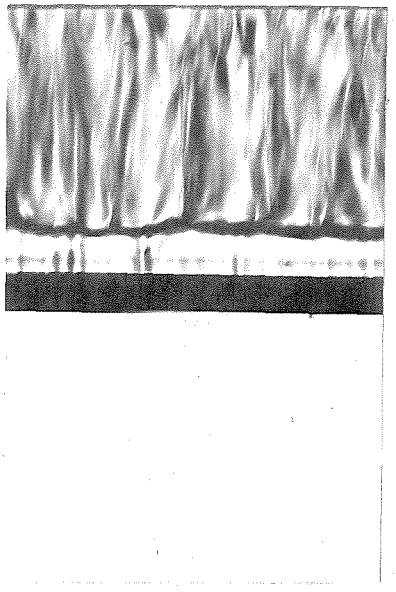

Station No. 69

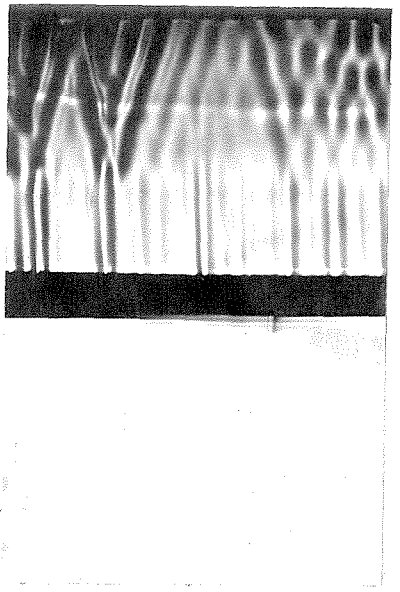

Station No. 72

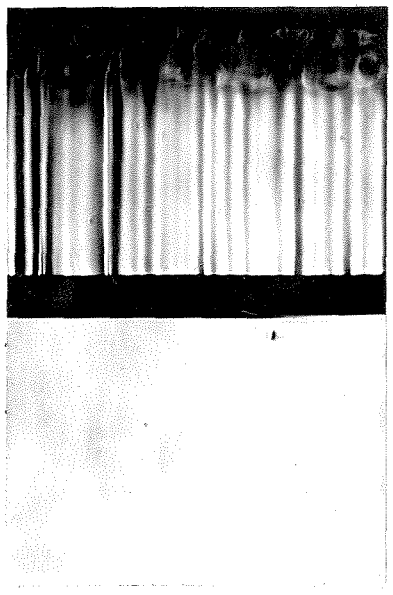

Station No. 74

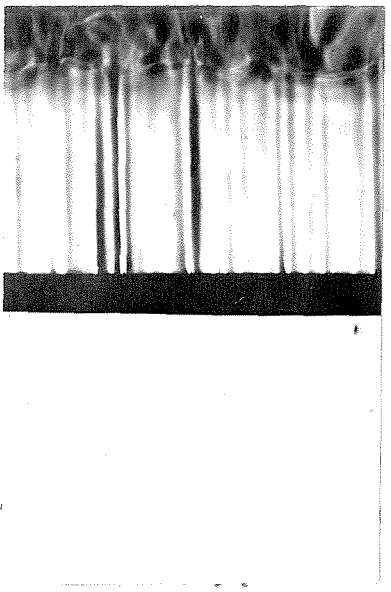

Station No. 76

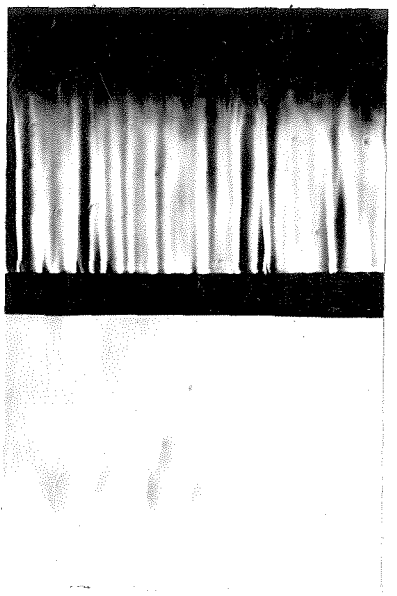

Station No. 77

FIGURE 12

HEAT TRANSFER RATE & HEAT TRANSFER COEFFICIENT vs. WIRE TEMPERATURE

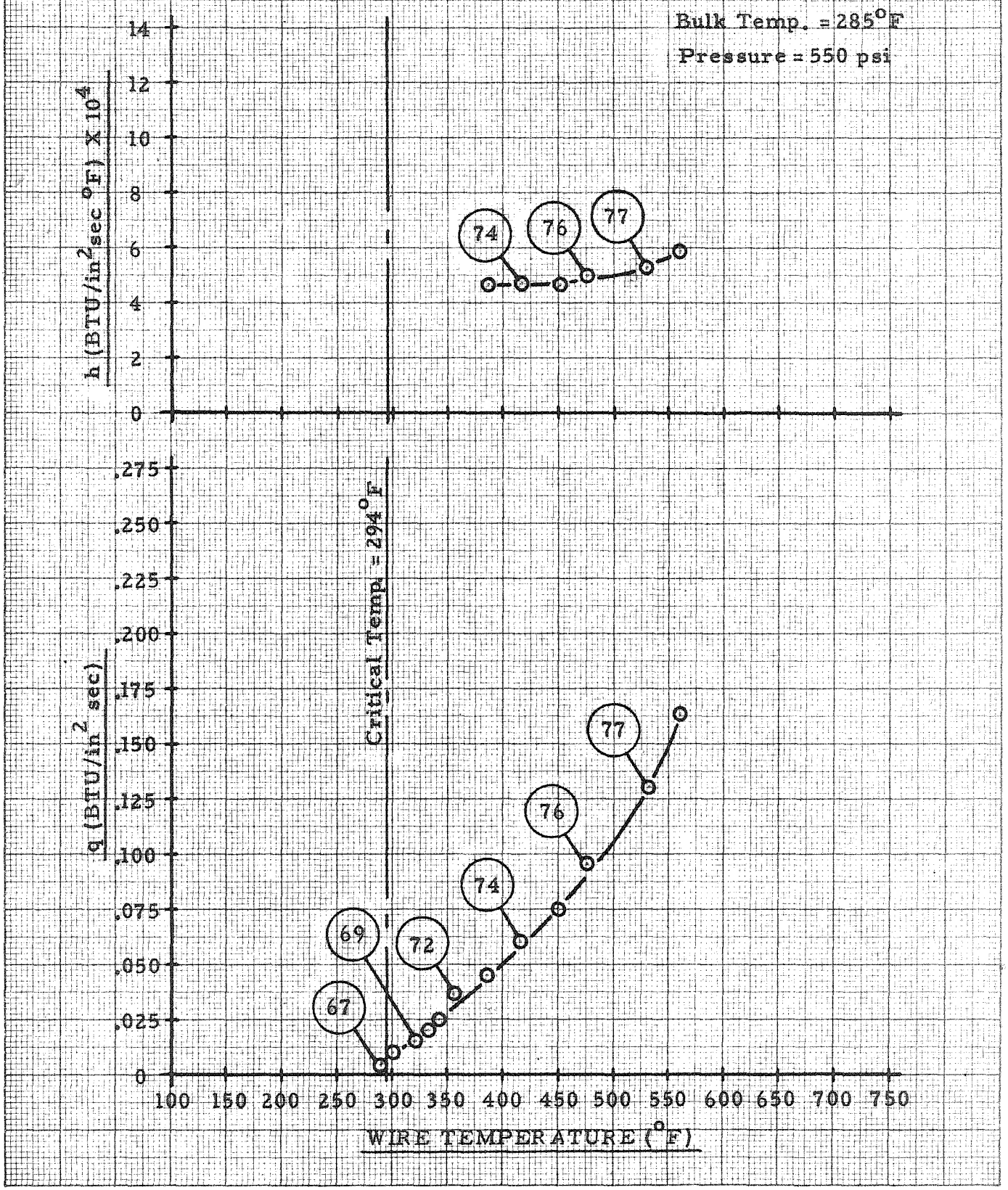

TEST RESULTS

Set VII

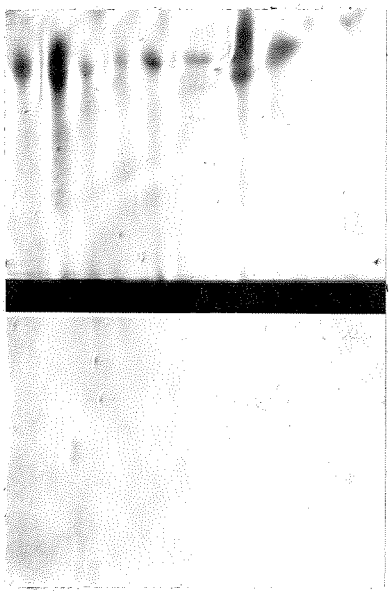

Station No. 79

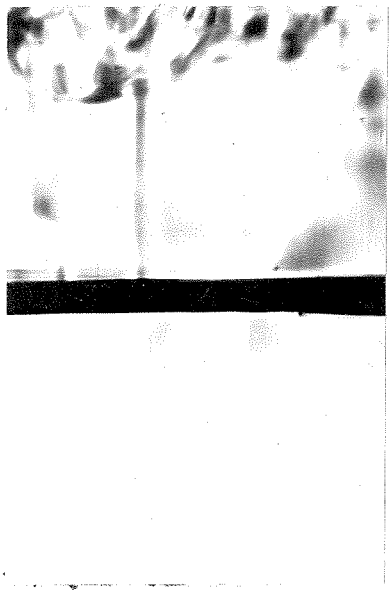

Station No. 81

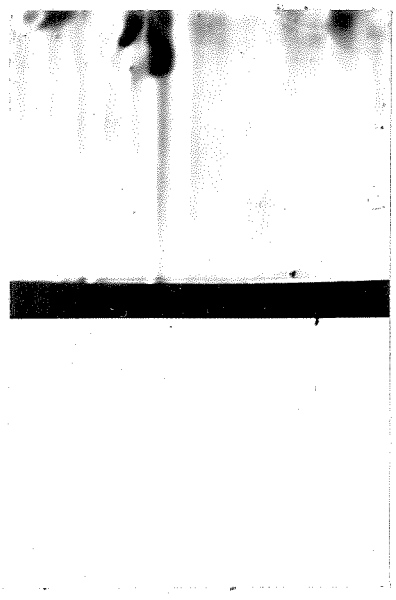

Station No. 85

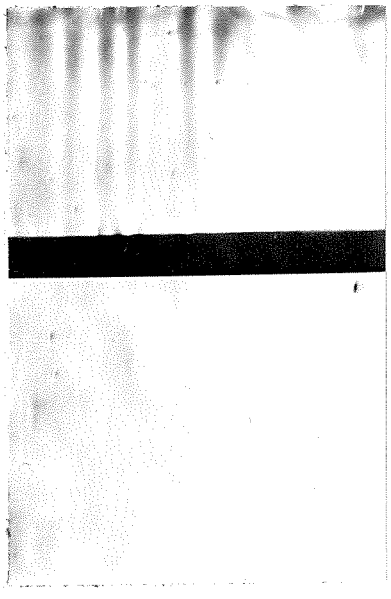

Station No. 87

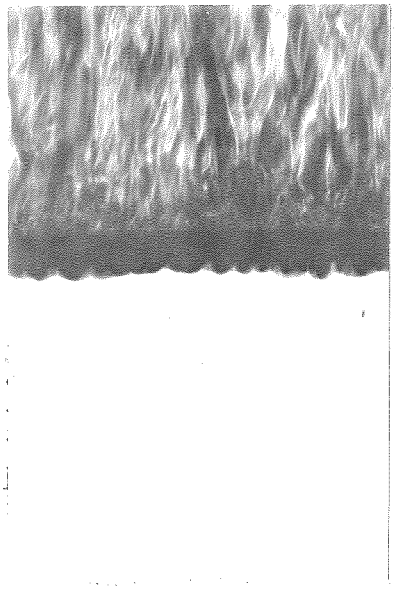

Station No. 88

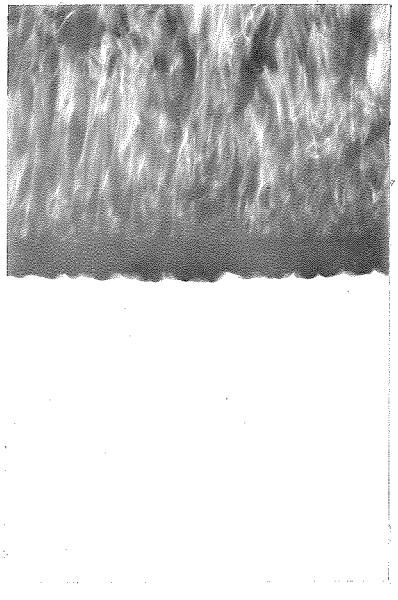

Station No. 89

FIGURE 13

HEAT TRANSFER RATE & HEAT TRANSFER COEFFICIENT
vs. WIRE TEMPERATURE

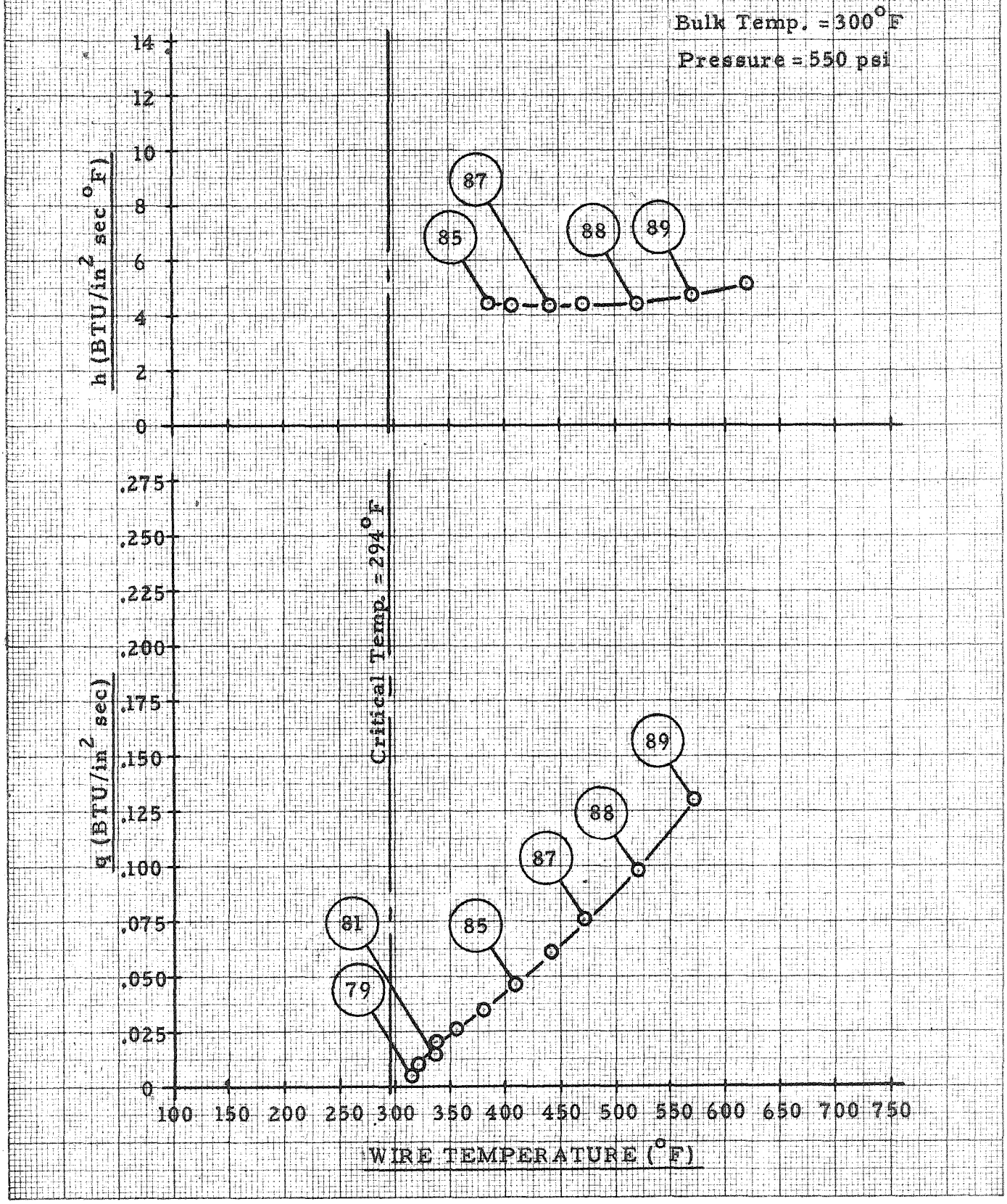

TEST RESULTS

Set VIII

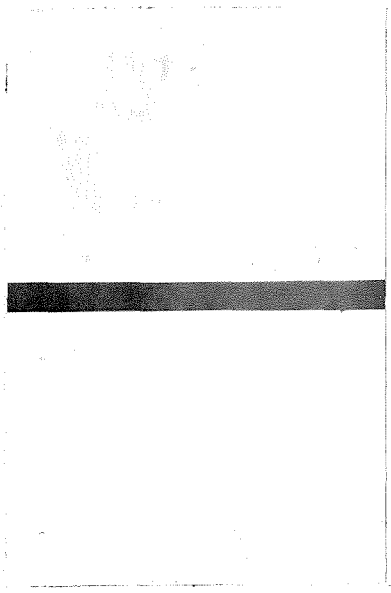

Station No. 91

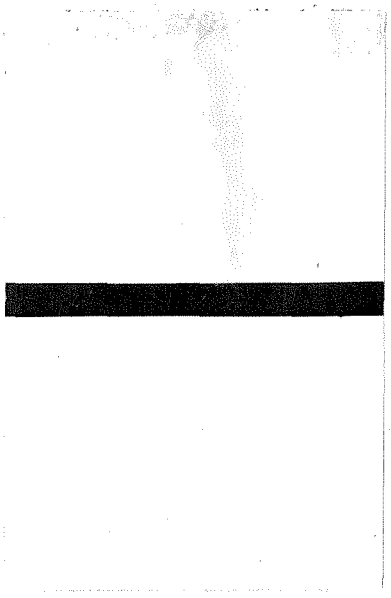

Station No. 93

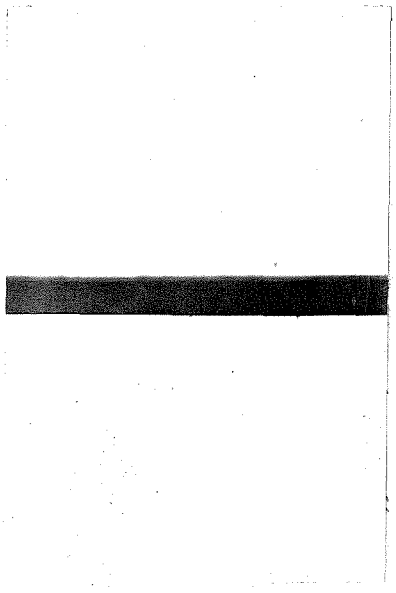

Station No. 96

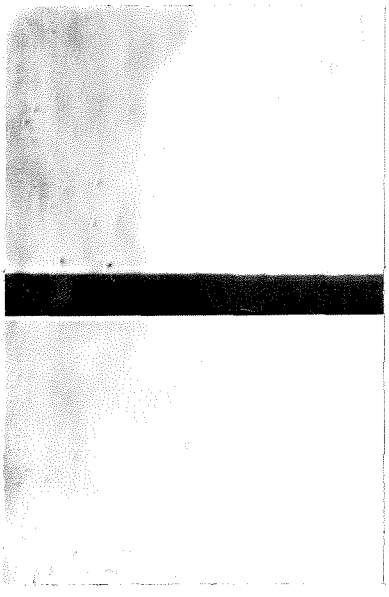

Station No. 98

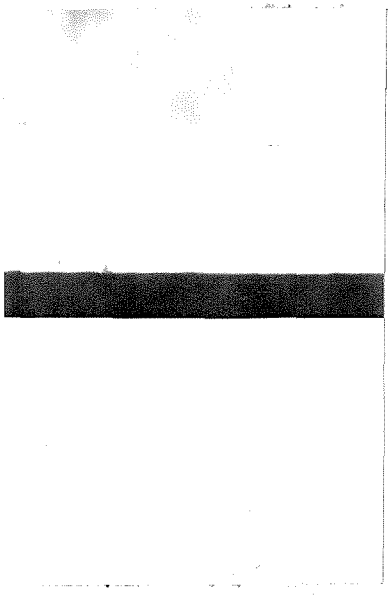

Station No. 100

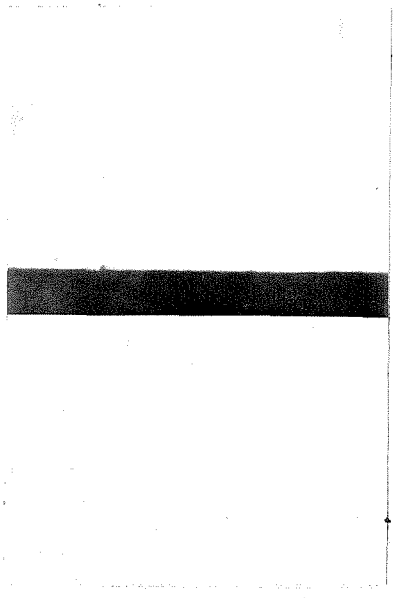

Station No. 101

FIGURE 14

HEAT TRANSFER RATE & HEAT TRANSFER COEFFICIENT
vs. WIRE TEMPERATURE

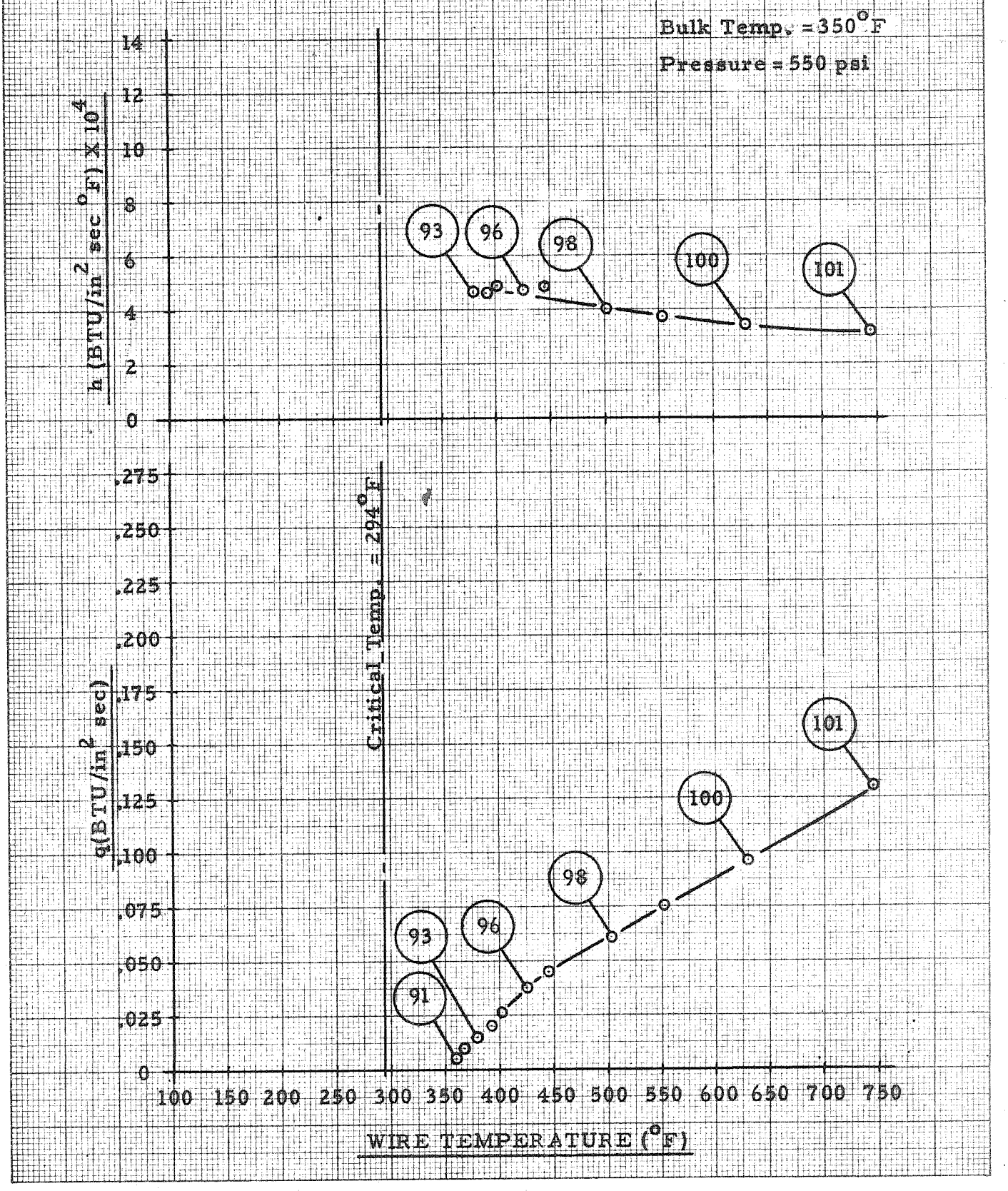

FIGURE 15

HEAT TRANSFER RATE vs. WIRE TEMPERATURE

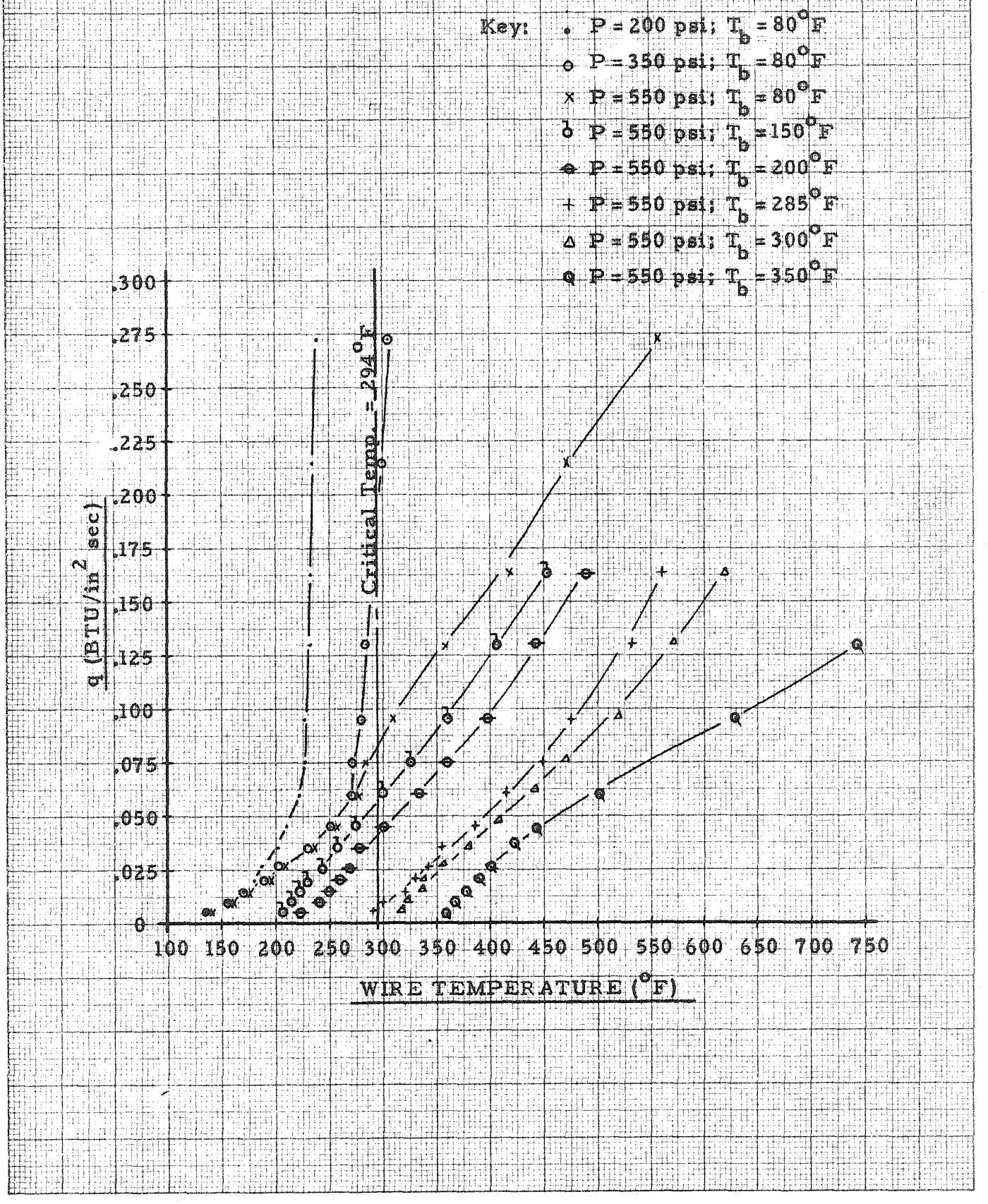

FIGURE 16

HEAT TRANSFER COEFFICIENT vs. WIRE TEMPERATURE

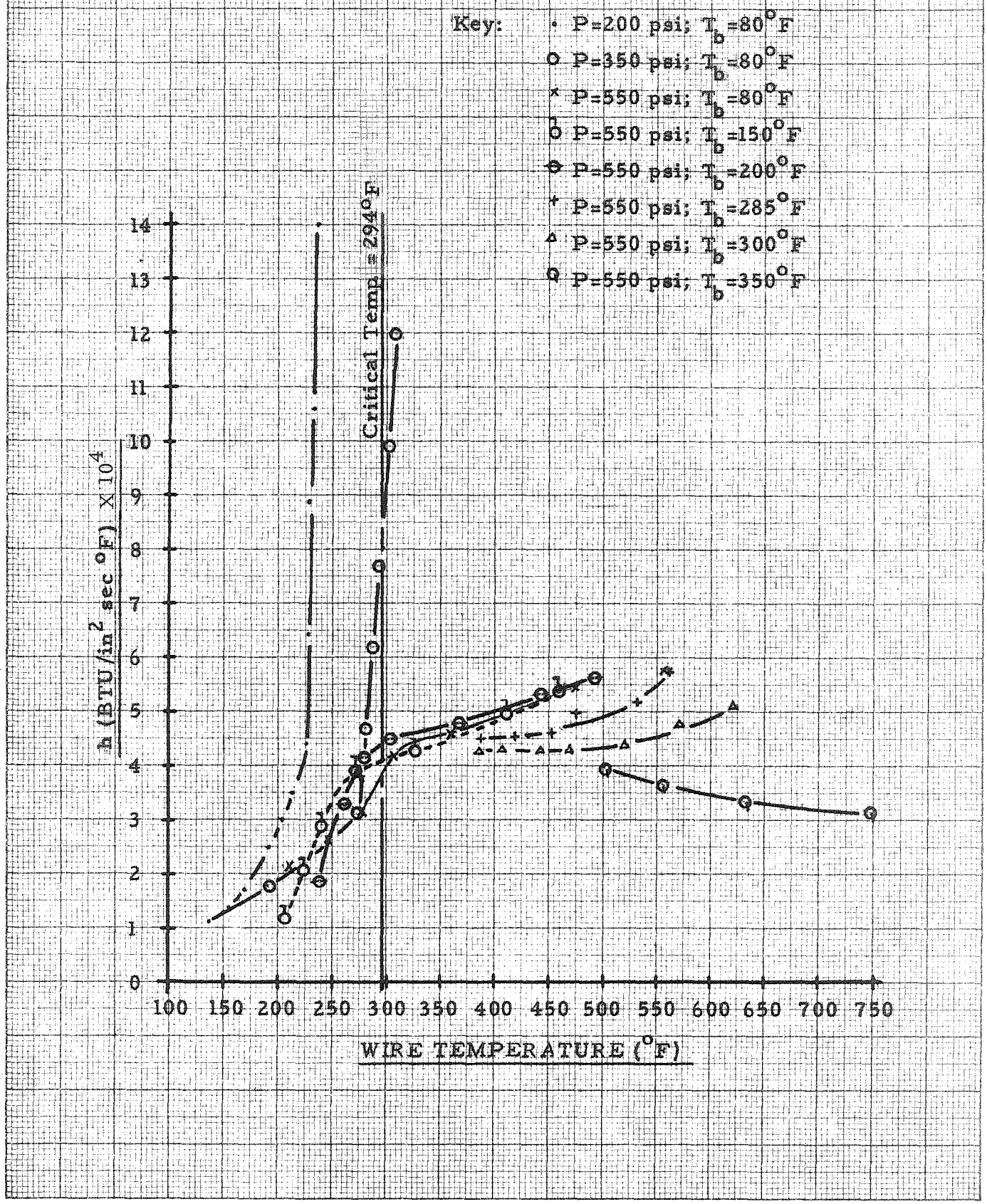

APPENDIX A

INSTRUMENT SENSITIVITY ANALYSIS

The purpose of this investigation is to determine the minimum change in temperature of the test wire that can be detected by measuring the change in resistance of the test wire.

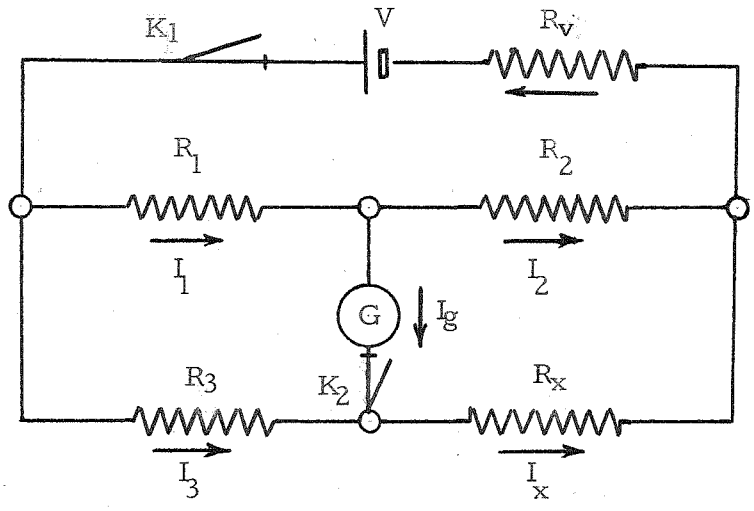

Figure 1A
The Wheatstone Bridge Network

Suppose that the resistances are such that with both keys closed no current flows in the galvanometer. Then, $I_g = 0$; $I_2 = I_1$; $I_3 = I_x$. The potentials C and D are necessarily equal so we have $I_1R_1 = I_3R_3$ and $I_1R_2 = I_3R_x$. Elimination of I_1 and I_3 gives

$$R_1R_x = R_2R_3 \quad \text{or} \quad \frac{R_1}{R_2} = \frac{R3}{R_x}$$

as the balance condition of the bridge. The balance condition does not involve the battery emf, V, the resistance R_g of the galvonometer, or the absolute values of R_1 and R_2. On the other hand, the current which

flows in the galvanometer when the bridge is slightly out of balance does depend on all of these quantities. Hence, the sensitivity of the bridge or the accuracy with which it will measure an unbalance requires a new computation. To carry this out it will be convenient to refer to Thevenin's theorem, a proof of which is given in many texts on electricity (9), and which states that any network as observed from two terminals, is equivalent to a source of emf in series with an impedance, the series combination being connected across the two terminals. To apply Thevenin's theorem to the bridge circuit, we may consider that the network of fig. 1A is enclosed in a box from which four terminals A, B, C, and D emerge as in fig. 2A. Then the theorem states that the entire effect of the network and the battery is equivalent, as far as any observation made at the terminals C and D are concerned, to a battery of emf, V_o, in series with a resistance R_o as shown in fig. 2A.

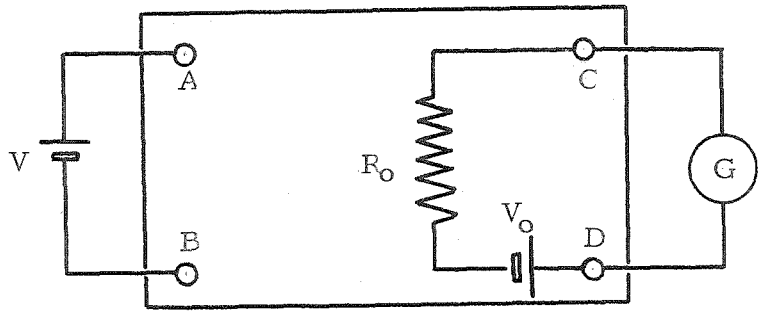

Figure 2A

Application of Thevenin's Theorem
to the Wheatstone Bridge

If the bridge is perfectly balanced, V_o is obviously zero. Suppose that this condition is not satisfied. Then we can find the magnitude of V_o by finding what the potential difference across the

terminals C-D may be with the external circuit open (i.e., with the galvanometer disconnected). Returning to fig. 1A we see that the difference with key K_2 open is

$$V_o = I_3R_3 - I_1R_1$$

In terms of battery emf V we have

$$I_1 = \frac{V}{R_1+R_2} \quad \text{and} \quad I_2 = \frac{V}{R_3+R_x}$$

I_g being zero with K_2 open. Substitution of these values shows that

$$V_o = \frac{V(R_2R_3-R_1R_x)}{(R_1+R_2)(R_3+R_x)}$$

To find R_o, we may ask what resistance would be observed between the terminals C and D, all emfs being absent.

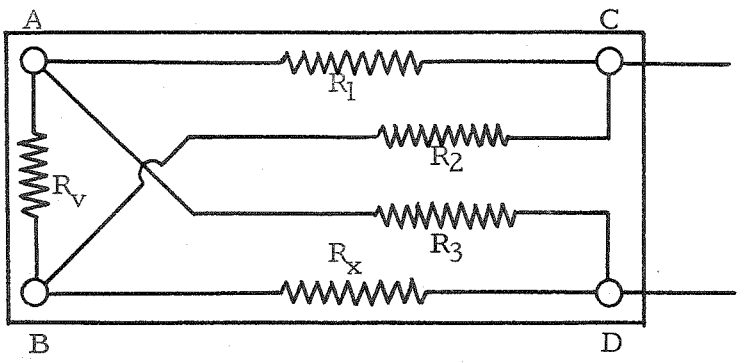

Figure 3A

Wheatstone Bridge Network
as viewed from Terminals C and D

It is clear from fig. 1A that the circuit as seen from C-D is that of fig. 3A where R_v indicates the internal resistance of the battery. In the test application a current source was used and R_v was equal to zero. Neglecting the resistance we have

$$R_o = \frac{R_1R_2}{R_1+R_2} + \frac{R_3R_x}{R_3+R_x}$$

$$= \frac{R_1R_2(R_3+R_x) + R_3R_x(R_1R_2)}{(R_1+R_2)(R_3+R_x)}$$

Finally, combining V_o and R_o, and remembering that the galvanometer is in series with R_o, we find that the current in the galvanometer is

$$I_g = \frac{V(R_2R_3 - R_1R_x)}{R_1R_2(R_3+R_x) + R_3R_x(R_1+R_2) + R_g(R_1+R_2)(R_3+R_x)}$$

The balance condition for the bridge is that $R_1R_x = R_2R_3$. We are particularly interested in the case when the bridge is almost exactly in balance, say when $R_x = \frac{R_2R_3}{R_1+\Delta R}$ where ΔR is very small compared to R_x. In this case,

$$(R_2R_3 - R_1R_x) = R_1\Delta R$$

If the galvanometer has a sensitivity S_i and a deflection d_{min} is the smallest that can be detected with reliability, we may set $I_g = \frac{d_{min}}{S_i}$ to show that the uncertainty in the measurement of R_x will be

$$\Delta R_{min} = \frac{d_{min}}{S_i V R_1} \left[R_g + \frac{R_1R_2(R_3+R_x) + R_3R_x(R_1+R_2)}{(R_1+R_2)(R_3+R_x)} \right]$$

The quantity ΔR_{min} is clearly a measure of the sensitivity of the bridge. Substituting the values of

$R_1 = R_3 = 0.623$ ohms
$R_2 = R_x = 0.600$ ohms
$V = I_x(R_3+R_x) = 1.223\, I_x$
$S_i = 1$ division/microampere
$d_{min} = 1/4$ division
$R_g = 978$ ohms

shows that the term $\frac{R_1R_2(R_3+R_x)+R_3R_x(R_1+R_2)}{(R_1+R_2)(R_3+R_x)}$

is negligible compared to R_g (978 compared to .407) and we obtain

$$\Delta R_{min} = \frac{0.480 \times 10^{-3}}{I_x}$$

For the experimental setup I_x limits the sensitivity. The sensitivity may be increased by increasing I_x. The smallest value of I_x used during test is

$$I_x = \frac{V}{R_V + 2.5} = \frac{120}{100 + 2.5} = 0.586 \text{ amperes}$$

where V represents line voltage and R_V represents the variable resistance in series with the bridge. The 2.5 ohms represents the combined resistance of the bridge and all the various lead wires. Using this value of I_x gives

$$\Delta R_{min} = 0.000818 \text{ ohms}$$

This is the smallest resistance change which can be detected by the bridge with the above current flowingthrough the bridge. As shown previously, ΔR_{min} decreases linearly with increasing current through the test wire. The minimum detectable temperature change may be calculated by the relationship

$$\Delta T_{min} = \frac{\Delta R_{min}}{R_x a}$$

where a is the thermal coefficient of resistivity. The thermal coefficient of resistivity for Nichrome wire was too small to measure accurately with available equipment. Therefore the quoted value of 0.00017 $\frac{\text{ohms}}{\text{ohms}}\,^{\circ}C$ in the Metals Handbook(7) was used. Substitution of this value into the above equation gives

$$\Delta T_{min} = 14.4\,^{\circ}F$$

APPENDIX B

BRIDGE CALIBRATION

It was shown in Appendix A that

$$\Delta R_{min} = \frac{d_{min}}{S_i V R_1} \left[R_g + \frac{R_1 R_2 (R_3+R_x) + R_3 R_x (R_1+R_2)}{(R_1+R_2)(R_3+R_x)} \right]$$

where the second term in this equation was negligible compared to R_g. It could be shown in the same manner that any general ΔR would be given by

$$\Delta R = 0.00199 \frac{I_g}{I_x}$$

where I_g is given in microamperes and I_x in amperes. The value of I_x changes as R_x changes and must be calculated as follows:

$$I_{total} = \frac{120}{R_V+2.5} = 1.835 \text{ for } R_V = 63$$
$$= 1.17 \text{ for } R_V = 100$$

where I_{total} is total current flowing into the bridge through series resistance R_V.

$$I_x = I_{total} \frac{R_1+R_2}{R_1+R_2+R_3+R_x} = I_{total} \frac{1.233}{1.846+R_x} = \frac{2.26}{1.846+R_x} \text{ for } R_V = 63 \text{ ohms}$$

$$= \frac{1.42}{1.845+R_x} \text{ for } R_V = 100 \text{ ohms}$$

The procedure for calibrating the bridge was to measure various resistances on a Kelvin Bridge, which was taken as a standard. (Leeds & Northrup, Serial No. 515588.) They were then measured on the Wheatstone Bridge and the values were compared. The results are given on the following pages.

The values agree very well except for a constant multiplying factor. If ΔR was set equal to

$$0.00184 \frac{I_g}{I_x}$$

instead of the calculated value of

$$0.00199 \frac{I_g}{I_x}$$

the agreement is almost perfect. This change in the multiplying constant indicates an error in the measurement of some bridge component such as R_g or may show the influence of lead resistances. This calibrated value of ΔR was used in calculating the test results.

RESULTS OF BRIDGE TEST

R_V	R_x	1.846+R_x	I_g	I_x	$\frac{I_g}{I_x}$	ΔR Calculated By Wheatstone Bridge	ΔR Measured on Kelvin Bridge	ΔR Calculated by Wheatstone Bridge Using Corrected Factor
63	.740	2.586	0	.874	0	0	0	0
63	.763	2.609	11	.867	12.7	.0252	.023	.0234
63	.793	2.639	26	.857	30.3	.0603	.057	.0558
63	.823	2.669	40	.847	47.2	.0940	.083	.087
63	.850	2.700	52	.837	62.2	.124	.110	.114
63	.883	2.729	66	.828	79.7	.158	.143	.146
63	.930	2.776	86	.815	105.5	.210	.190	.196
63	.946	2.820	100	.802	12.5	.249	.224	.230
100	.750	2.596	0	.548	0	0	0	0
100	.801	2.647	15	.537	28.0	.0567	.051	.0515
100	.865	2.711	33	.524	63.0	.125	.115	.116
100	.897	2.743	41	.518	79.2	.158	.147	.146
100	.955	2.801	56	.507	110.	.219	.205	.202
100	.999	2.845	68	.492	136	.270	.249	.250
100	1.12	2.966	96	.479	200	.389	.370	.368

To correct bridge by constant multiplying factor

let $\Delta R = \frac{0.00199}{1.08} \frac{I_g}{I_x}$

$$\Delta R = 0.00184 \frac{I_g}{I_x}$$

GRAPHICAL RESULTS OF BRIDGE CALIBRATION

$R_V = 63$ Ohms

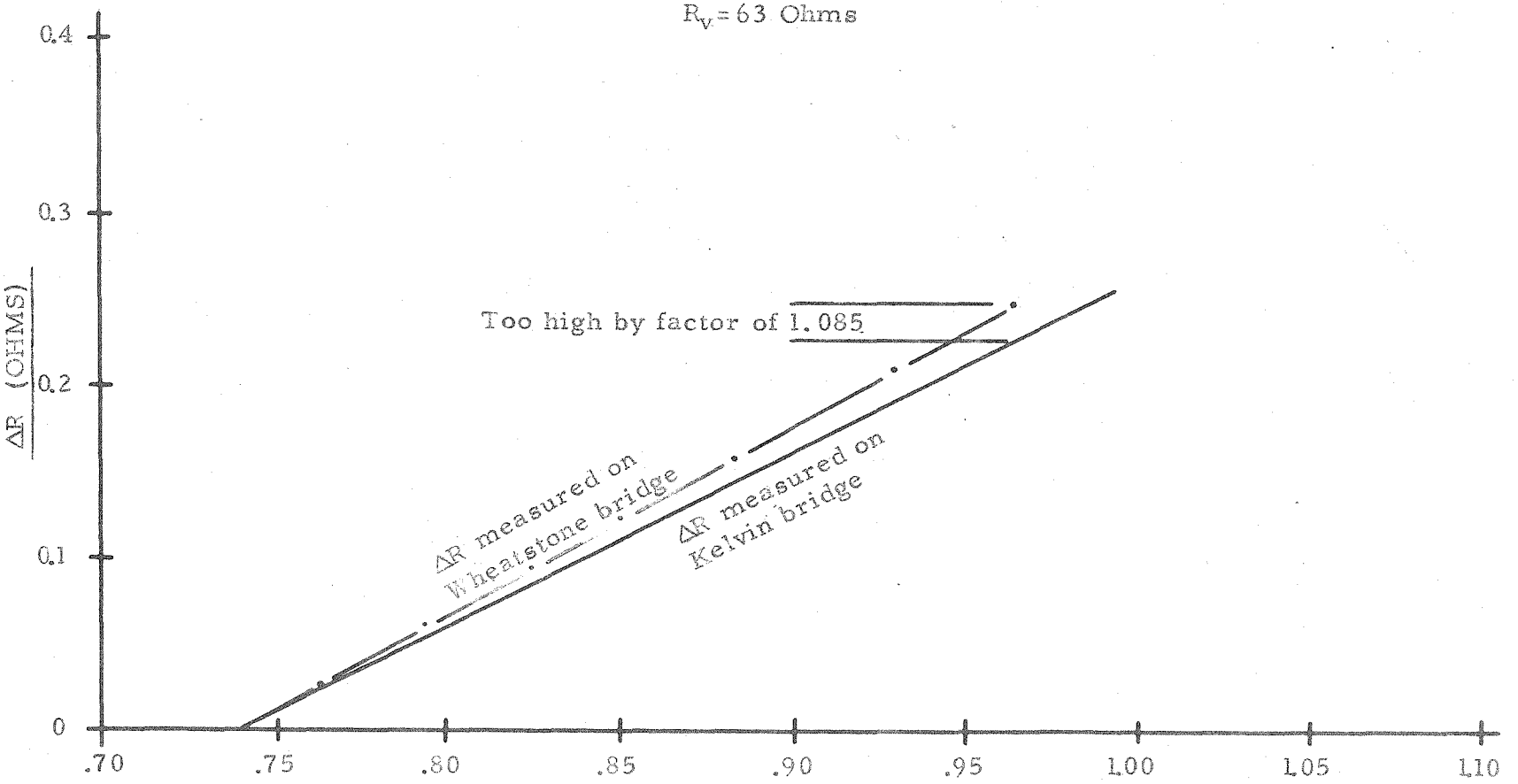

GRAPHICAL RESULTS OF BRIDGE CALIBRATION

R_V=100 Ohms

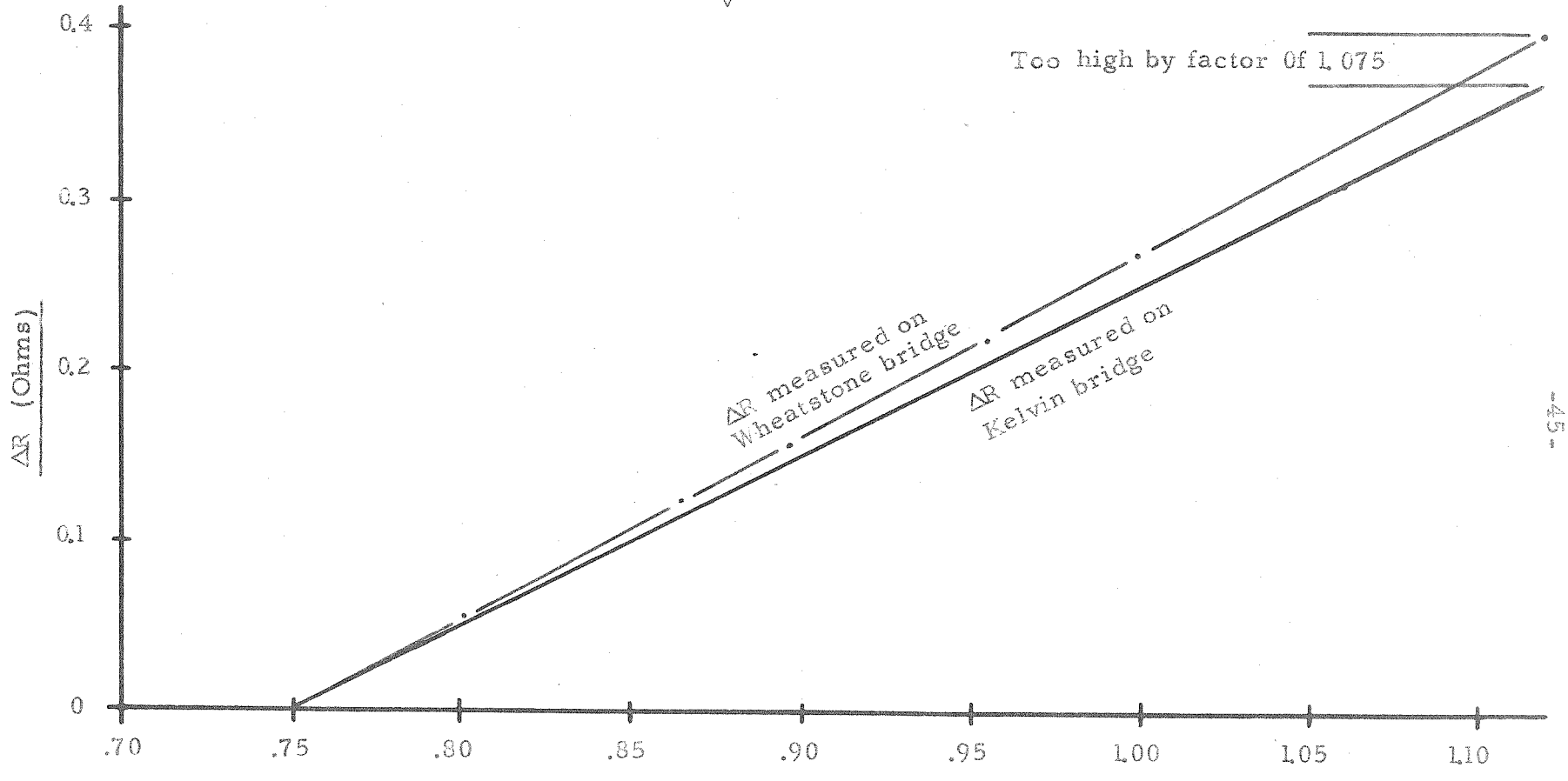

APPENDIX C

SAMPLE CALCULATION

Experimental Set IV

Station No. 54

Fluid Bulk Temperature 150°F

Fluid Pressure 550 psi

Line Voltage, V, = 120V

Wire Resistance, R_x = 0.600 ohms

Wire Length, L, = 1.0 in.

Wire Diameter, d, = 0.010 in.

Readings: Rheostat, R_V = 17.5 ohms
Microammeter I_g = 34.50 microamperes

Heat energy dissipated by the wire may be equated to electrical energy absorbed.

$$q\left(\frac{BTU}{in^2\ sec}\right) = \frac{I_x^2 R_x}{\pi d L}\left(\frac{watts}{in^2}\right) .000950\left(\frac{BTU/sec}{watt}\right)$$

$$q = \frac{0.600}{\pi\,(.010)(1.0)}\ .000450\ I_x^2\left(\frac{BTU}{in^2\ sec}\right) = 0.0181\ I_x^2\left(\frac{BTU}{in^2\ sec}\right) \quad (1)$$

The current flowing through the test wire I_x is one-half the current flowing through the rheostat. The current through the rheostat is equal to the line voltage divided by the sum of resistance of the rheostat and the combined resistance of the bridge and lead wires which appear in series with the rheostat. The resistance of the bridge and lead wires was measured and found to be 2.5 ohms.

$$I_x = \frac{V}{2(R_V + 2.5)} = \frac{120}{2(17.5+2.5)} = \frac{120}{40} = 3.00 \text{ amperes}$$

Substitution of this value of I_x into Equation 1 gives

$$q = 0.163\ \frac{BTU}{in^2\ sec}$$

In Appendix B it was shown that

$$\Delta T = 0.00184 \frac{I_g}{I_x}$$

Substitution of the recorded value of I_g and the calculated value of I_x gives

$$\Delta T = 0.00184 \frac{34.50}{3.00} = 372\ ^{o}F$$

Since this ΔT is measured on a bridge calibrated to give no temperature difference at a wire temperature of 80 ^{o}F, the wire temperature is

$$T_w = 372 + 80 = 452\ ^{o}F$$

APPENDIX D

DETERMINATION OF HEAT TRANSFER RATES

$$I_x = \frac{V}{2R} = \frac{120}{2(R_V + 2.5)} = \frac{60}{R_V + 2.5}$$

$R_x = 0.600$ ohms

$$q = 0.0181\, I_x^2 \left(\frac{BTU}{in^2\, sec}\right)$$

R_V	$R_V + 2.5$	I_x	I_x^2	q
100	102.5	.586	.343	.0062
78	80.5	.747	.557	.0101
63	65.5	.914	.835	.0151
55	57.5	1.04	1.08	.0196
47	49.5	1.21	1.46	.0264
40	42.5	1.41	1.99	.0360
35	37.5	1.60	2.56	.0464
30	32.5	1.84	3.38	.0612
27	29.5	2.03	4.12	.0746
23.5	26.0	2.30	5.29	.0958
20	22.5	2.67	7.12	.129
17.5	20.0	3.00	9.00	.163
15	17.5	3.43	11.7	.216
13	15.5	3.87	15.0	.272
11.5	14.0	4.28	18.3	.332

APPENDIX E

TABULATED TEST RESULTS

		$T_b = 80^oF$ P = 200 psi			$T_b = 80^oF$ P = 350 psi		
R_v	q	Station Number	I_g	ΔT	Station Number	I_g	ΔT
100	.0062	1	1.00	55	15	1.00	55
78	.0101	2	1.75	76	16	1.75	76
63	.0151	3	2.50	89	17	2.50	89
55	.0196	4	3.25	102	18	3.50	109
47	.0264	5	4.00	107	19	4.50	120
40	.0360	6	5.25	121	20	6.50	149
35	.0464	7	6.50	132	21	8.50	172
30	.0612	8	8.00	141	22	10.75	190
27	.0746	9	9.25	148	23	12.00	192
23.5	.0958	10	10.50	148	24	14.00	198
20	.129	11	12.50	153	25	17.00	206
17.5	.163	12	14.00	153	26	19.50	210
15	.216	13	15.50	156	27	23.00	218
13	.272	14	19.00	160	28	26.00	227

		$T_b = 80^oF$ P = 550 psi			$T_b = 150^oF$ P = 550 psi		
R_v	q	Station Number	I_g	ΔT	Station Number	I_g	ΔT
100	.0062	29	1.00	55	43	2.25	125
78	.0101	30	1.75	76	44	3.00	131
63	.0151	31	2.50	89	45	4.00	142
55	.0196	32	3.50	109	46	4.75	148
47	.0264	33	4.50	120	47	6.00	161
40	.0360	34	6.50	149	48	7.50	173
35	.0464	35	8.50	172	49	9.25	188
30	.0612	36	11.00	193	50	12.75	216
27	.0746	37	12.75	204	51	16.25	244
23.5	.0956	38	16.25	229	52	20.00	280
20	.129	39	23.00	279	53	27.00	327
17.5	.163	40	31.50	340	54	34.50	372
15	.216	41	41.00	390			
13	.272	42	57.00	478			

		$T_b = 200^oF$ P = 550 psi			$T_b = 285^oF$ P = 550 psi		
R_v	q	Station Number	I_g	ΔT	Station Number	I_g	ΔT
100	.0062	55	2.75	152	67	3.75	208
78	.0101	56	3.75	163	68	5.00	218
63	.0151	57	4.75	169	69	6.75	240
55	.0196	58	5.75	179	70	8.00	250
47	.0264	59	7.00	188	71	9.75	261
40	.0360	60	8.75	201	72	12.00	276
35	.0464	61	11.00	223	73	15.00	305
30	.0612	62	14.50	255	74	19.00	335
27	.0746	63	17.50	280	75	23.00	368
23.5	.0958	64	22.50	317	76	28.00	395
20	.129	65	30.00	363	77	37.00	448
17.5	.163	66	38.00	410	78	44.50	480

		$T_b = 300^oF$ P = 550 psi			$T_b = 350^oF$ P = 550 psi		
R_v	q	Station Number	I_g	ΔT	Station Number	I_g	ΔT
100	.0062	79	4.25	236	91	5.00	278
78	.0101	80	5.50	239	92	6.50	282
63	.0151	81	7.25	258	93	8.50	302
55	.0196	82	8.25	258	94	10.00	312
47	.0264	83	10.25	274	95	12.00	322
40	.0360	84	13.00	299	96	15.00	345
35	.0464	85	16.00	325	97	18.00	365
30	.0612	86	20.50	361	98	24.00	422
27	.0746	87	24.50	392	99	29.50	472
23.5	.0958	88	31.00	437	100	39.00	550
20	.129	89	40.50	490	101	55.00	665
17.5	.163	90	50.00	540			

APPENDIX F
TABLE OF SOME SIGNIFICANT PHYSICAL PROPERTIES OF FREON 114A

Chemical Formula	$C_2Cl_2F_4$
Molecular Weight	170.9
Boiling Point (^{o}F) at 1 Atmosphere Pressure	37.6
Freezing Point (^{o}F) at 1 Atmosphere Pressure	-76
Critical Temperature (^{o}F)	294
Critical Pressure (psi absolute)	478
Saturated Liquid Viscosity at 86 ^{o}F (cp)	0.440
Vapor Viscosity at 86 ^{o}F & 1 Atmosphere Pressure (cp)	0.0103
Saturated Liquid Density at 86 ^{o}F (lbs/ft^3)	90.54
Saturated Vapor Density at 86 ^{o}F (lbs/ft^3)	1.191
Latent Heat of Vaporization at 5 ^{o}F (BTU/lb)	60.2
Specific Heat of Liquid at 86 ^{o}F (BTU/lb. ^{o}F)	0.23
Specific Heat of Vapor at 1 Atmosphere Pressure and 86^{o}F (BTU/lb. ^{o}F)	0.16
Specific Heat Ratio at 86 ^{o}F & 1 Atm. (k=Cp/Cv)	1.01
Thermal Conductivity of Liq. at 86 ^{o}F (BTU ft/ft^{2}hr. ^{o}F)	Unknown
Thermal Conductivity of Vapor at 86 ^{o}F(BTU ft/ft^{2}hr. ^{o}F)	0.0054
Toxicity	Very Low
Flammability and Explosivity	None
Odor	Ethereal
Water Solubility in Liq. Freon at 86 ^{o}F (gms/100gms. Refrig)	0.0057
Miscibility with Lubricating Oils	Partial

REFERENCES

1. Doughty, D. L. and Drake, R. M., "Free Convection Heat Transfer from a Horizontal Right Circular Cylinder to Freon 12 Near the Critical State", ASME Transaction 78, 1843-1850 (1956).

2. Powell, W. B., "Heat Transfer to Fluids in the Region of the Critical Temperature", Progress Report No. 20-285, Jet Propulsion Laboratory, California Institute of Technology, Pasadena, California, 1956, pp. 1-70.

3. Dickinson, N. L. and Welch, C. P., "Heat Transfer to Super Critical Water", ASME Paper No. 57-Ht-7, 1957, pp. 1-7.

4. Deissler, R. G., "Heat Transfer and Fluid Friction for Fully-Developed Turbulent Flow of Air and Supercritical Water with Variable Fluid Properties", ASME Transactions 76, 73-85 (1954).

5. Bringer, R. P. and Smith, J. M., "Heat Transfer in the Critical Region", J. AIChE 3, 149 (1957).

6. Handbook of Chemistry and Physics, Fourteenth Edition, Chemical Rubber Publishing Company, Cleveland, Ohio, 1958, p. 2954.

7. Metals Handbook, American Society for Metals, Cleveland, Ohio, 1948, p. 1060.

8. Ellion, M. E., "A Study of the Mechanism of Boiling Heat Transfer", Jet Propulsion Laboratory, Memo No. 20-28, March, 1954.

9. Harnwell, G. P., Principles of Electricity and Electromagnetism, Second Edition, McGraw-Hill, New York, 1949, pp. 120-123.

10. General Chemical Division, Allied Chemical & Dye Corporation, Genetron Technical Data Bulletin 114a-1-58, New York, 1958.